



Wind-driven Rain Study in the Coastal Climate of British Columbia
Final Report

Submitted to:

Mr. Silvio Plescia, P.Eng.
Sustainable Housing and Communities
Policy and Research Division
Canada Mortgage and Housing Corporation
700 Montreal Road
Ottawa, Ontario
K1A 0P7

Dr. Denisa Lonescu
Manager, Research and Education
Homeowner Protection Office
PO Box 11132, Royal Centre
Suite 2270
1055 W. Georgia Street
Vancouver, British Columbia
V6E 3P3

Mr. Brian Simpson
British Columbia Housing Management Commission
800 – 5945 Kathleen Avenue
Burnaby, British Columbia
V5H 4J7

Prepared by:
Hua Ge, Ph.D., P. Eng.
Ronald Krpan, P. Eng.
Building Science Centre of Excellence
British Columbia Institute of Technology
3700 Willingdon Ave.
Burnaby, British Columbia
V5G 3H2

Acknowledgement

The authors would like to acknowledge the financial support and direction provided by the Canada Mortgage and Housing Corporation and the British Columbia Homeowner Protection Office. The School of Construction and the Environment of the British Columbia Institute of Technology provided significant financial and in-kind contributions for this project. We would also like to thank the British Columbia Housing Management Commission and the British Columbia Affordable Housing Society for allowing us to access their buildings.

The authors are grateful for the guidance and valuable input provided by Dr. Michael Lacasse from the National Research Council of Canada and Mr. Alan Dalglish.

Executive Summary

The quantity and spatial distribution of wind-driven rain are important considerations for building envelope design; however, there is limited information on the rain load to which the building envelope is exposed during its service life. To better inform the design process for walls, measurements on buildings especially in the southwest region of British Columbia, a region characterized by a diverse microclimate and frequent instances of wind-driven rain over the winter season, are desired.

The objectives of this study are to quantify the amount of rain impinged on typical building wall surfaces, to establish the influence of overhang on wind-driven rain exposure, and to verify the empirical method of quantifying wind-driven rain based on comparisons to new measurements at various locations in Metro Vancouver. Eight buildings were chosen for this study to reflect a variety of construction types, building geometries, and surrounding topographies. Buildings with both sloped and flat roofs and buildings with and without roof overhangs were included for comparative purposes. The parameters monitored include local weather data, i.e., wind speed, wind direction, and horizontal rainfall, and driving rain on the façade. In general, six to eight driving rain gauges were installed on each selected building. The majority of these driving rain gauges were installed on the east and south façades, corresponding to the prevailing wind-driven rain direction in the BC Lower Mainland. Data were collected from November 2006 to July 2008.

The data analyses include on-site wind and rain conditions, Driving Rain Index (DRI), spatial distribution of wind-driven rain on wall surfaces, and the effect of overhang. The applicability of using an empirical method to quantify wind-driven rain on specific wall surfaces is also examined. The main conclusions drawn from this study include:

- The airfield Driving Rain Index calculated using wind speed, wind direction, and horizontal rainfall intensity is only a relative indicator of the potential wind-driven rain exposure of a specific wall, and the actual amount of driving rain impinged on the surface is largely influenced by the building geometry and design details, i.e. overhang.
- The prevailing wind direction varies from site to site. Buildings 2, 3, 5 and 7 are located in the Vancouver region. The prevailing wind direction is from the east with a slightly lower frequency of wind from the east-north-east for Buildings 2 and 3 and from the northeast for Buildings 5 and 7, although the wind direction at the Vancouver International Airport is distinctly from the east. For buildings located in the Burnaby region, the prevailing wind direction is from the east-south-east for Building 1 (8), and from the east with a second highest frequency of wind from the south-south-east for Building 6.
- The average wind speed recorded is mild, less than 2 m/s for low-rise buildings, except for Building 3. Building 3 has a higher wind speed in the range of 2-4m/s. The two high-rise buildings recorded an average wind speed slightly less than 4 m/s. Most of the time, wind speed is within the range of 2–6 m/s. In general, the average wind speed is slightly higher during rain hours; however, the maximum wind speed recorded during rain hours is lower than that during all hours. The average wind speed varies slightly over seasons and the wind speed is the highest during the winter. The total amount of rainfall varies slightly from site to site. The average rainfall intensity recorded during the monitoring period falls under 2 mm/hr.
- In general, the east and southeast facing walls have the highest wind-driven rain exposure. For some building sites monitored, walls facing northeast and north may receive a comparably high

amount of rain. Therefore, these walls may have a higher risk of moisture damage due to the much lower solar radiation received on a north or northeast facing wall.

- The amount of driving rain impinged on the wall surface is small compared to the literature data, probably due to the mild wind and light to moderate rain in this particular climate. The driving rain impinged on low-rise buildings with an overhang ratio of about 0.04 is only about 2–4% of the horizontal rainfall, and a significantly higher amount of 11% may be expected for low-rise buildings without any overhang. The 6-storey medium-height building receives an average amount of driving rain of about 15% of the horizontal rainfall, and a 16-storey high-rise building receives about 13% of the horizontal rainfall.
- The measured data show that the overhang reduces wind-driven rain exposure by about four times for low-rise buildings and one and a half times for high-rise buildings for an overhang with a ratio of 0.04. Given that the higher amount of driving rain received by high-rise buildings is due to the high rain deposition at the upper part of the building while the lower part receives a small amount due to the blocking effect, the provision of an overhang may be effective for high-rise buildings in this particular climate.
- The use of weather data reported from the Vancouver International Airport generally underestimates the amount of wind-driven rain received by all monitoring buildings except for Building 2. The use of weather data from the close-by GVRD Burnaby South station significantly improves the accuracy in estimating the amount of wind-driven rain on Buildings 3 and 6. For Building 2, the use of weather data from the close-by Kitsilano station results in slightly better results than using the weather data from the airport station. Therefore, direct measurements of the rain impacting on building façades should be made wherever possible in southern BC, a region characterized by significant local variation of wind and rain conditions. When direct measurements are not available, data from a weather station located in the proximity of the building site with similar surroundings should be used, such as data collected from the GVRD's ambient air quality monitoring network. When weather data from the Vancouver International Airport is used for buildings in the Vancouver region, significant errors could be introduced, especially when the on-site prevailing wind direction is different from the prevailing wind direction at the airport station.

Table of Contents

1.	Introduction.....	6
2.	Description of selected buildings and monitoring protocol.....	6
2.1.	Building selection	6
2.2.	Instrumentation and sensor locations.....	9
3	Data collection	11
4	Data Analysis.....	14
4.1.	On-site wind and rain conditions	14
4.2.	Airfield Driving Rain Index.....	17
4.3.	Spatial distribution of wind-driven rain on the façade.....	21
4.4.	Effect of overhang.....	26
4.5.	Assessment of wind-driven rain on wall surfaces using empirical correlations	28
5	Conclusions.....	32
6	References.....	35
	Appendix A.....	36

1. Introduction

The amount of driving rain received by the building envelope is an important environmental load for building envelope design; however, there is limited information on the rain load to which the building envelope is exposed during its service life. To date, most of the research effort in Canada has focused on assessing the wind-driven rain exposure of a region using historical meteorological data recorded at weather stations rather than the wind-driven rain exposure of a specific building. The actual driving rain load received by building façades is also influenced by the building geometry and design details, for example, the size of overhang. However, there is very limited quantitative information on the influence of design details on the wind-driven rain exposure.

Current best practice guidelines for building envelope wall assemblies lead the user to identify exposure conditions for wind-driven rain in order to select an appropriate type of assembly, especially in the coastal climate of British Columbia (BC). Because of a lack of data, current practice depends on professional judgment. The amount of wind-driven rain that impinges on the façades of buildings can be quantified using driving rain gauges. While some buildings in coastal BC have been fitted with driving rain gauges in the recent past, only a few gauges were typically used on each building.

To bridge the knowledge gap, an inventory of buildings in the BC Lower Mainland are instrumented to collect wind-driven rain data and quantify the influence of building geometry on rain wetting on façades. This research project aims to:

- Collect wind-driven rain data on a number of strategically selected buildings in the coastal BC climate to bridge the gap in wind-driven rain data available in Canada;
- Verify and extend the wall factors described in existing publications to cover more building geometries;
- Verify the procedure prescribed by the British Standard to correlate the weather data recorded at meteorological stations to specific building sites;
- Establish the influence of overhang size on wind-driven rain exposure of buildings;
- Provide experimental data to validate Computational Fluid Dynamics (CFD) models.

This report provides a summary of the buildings selected, the instrumentation protocol, data collection, and the results of data analysis.

2. Description of selected buildings and monitoring protocol

2.1. Building selection

In total, 35 buildings from the housing stock of the BC Housing Management Commission (BCHMC) were evaluated for their potential use in this study. Most of these buildings are located in the Vancouver region with a small number in the regions of Richmond, Burnaby, Surrey and North Vancouver. The original plan also called for a 3-storey or 4-storey residential building in the high rainfall region of the North or West Vancouver; however, no suitable building was identified at the time. After reviewing the buildings and their surroundings, eight buildings were chosen for the two-year monitoring, as listed in Table 1. Effort was made to choose buildings with a higher wind-driven rain exposure. The location of these buildings is shown in Figure 1.

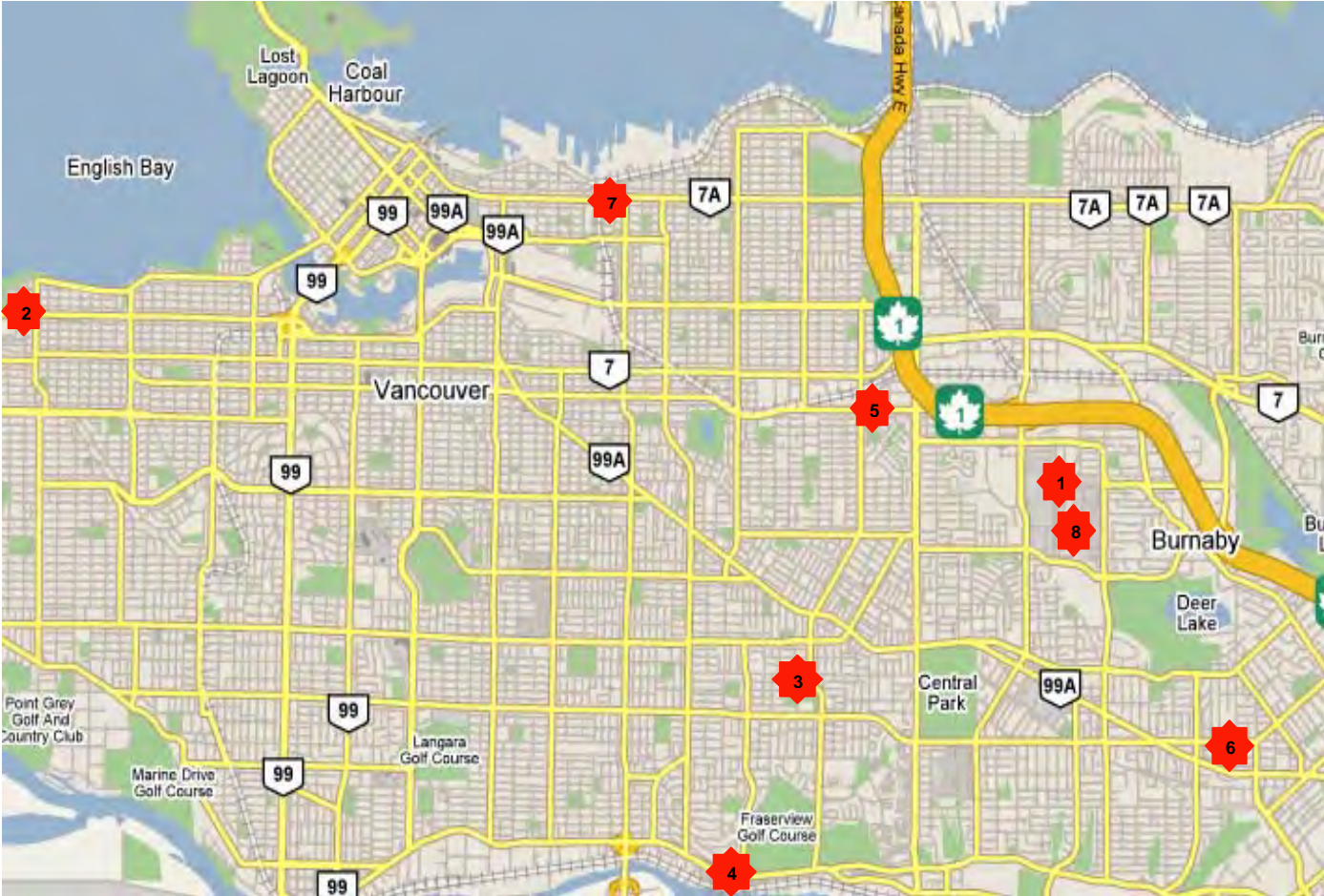



Figure 1. Location of subject buildings monitored for the wind-driven rain project.

Table 1. General description of buildings monitored.

Site	Construction type	Geometry	Obstruction	Region	Available buildings
Bldg. 1	two-storey single family	sloped roof with 1' (0.3 m) overhang	sheltered	BCIT Burnaby Campus	
Bldg. 2	three-storey multi-unit residential	flat roof without overhang	moderate	Vancouver Jericho beach Within 1 km of direct water exposure	
Bldg. 3		low-sloped roof with 1' (0.3 m) overhang		Vancouver	
Bldg. 4	four-storey multi-unit residential	sloped roof with 1' (0.3 m) overhang	exposed	along Fraser River in Vancouver region	
Bldg. 5	six-storey medium height residential	flat roof without overhang	moderate	Vancouver	
Bldg. 6	sixteen storey high-rise	flat roof without overhang	moderate	Burnaby	
Bldg. 7	twelve-storey high-rise	flat roof with 3' (0.9 m) overhang	moderate	Vancouver	
Bldg. 8	single-storey long aspect ratio building	flat roof with 6" (0.15 m) overhang	moderate	BCIT Burnaby Campus	

2.2. Instrumentation and sensor locations

The parameters monitored include local weather data, i.e., wind speed, wind direction, and horizontal rainfall, and driving rain on the façade. Some buildings are instrumented with relative humidity and temperature probes as well. In general, six to eight driving rain gauges were installed on each selected building. The majority of these driving rain gauges were installed on the east and south façades, corresponding to the prevailing wind-driven rain direction in the BC Lower Mainland.

Wind

The on-site wind speed and wind direction are measured at 3 m above the roof surface. To minimize the effect of local turbulence induced by the building, the weather mast was placed in the centre of the roof. The wind monitor used has a propeller type anemometer with a range of 0–60 m/s to measure wind speed and a wind vane measuring wind direction in the range of 0 to 355°.

Rain

The ideal placement of the horizontal rain gauge on the ground away from obstruction is difficult to implement in complex residential areas. In this study, the horizontal rainfall is measured by a tipping bucket rain gauge placed on top of the roof, located as close to the centre as possible to minimize the error introduced by the local turbulence and wind deformation. The wind error is considered to be the most important error source in horizontal rainfall measurements due to the systematic deformation of the wind flow above the gauge orifice and, hence, of the raindrop movements in this flow by the presence of the gauge body itself. Other errors associated with horizontal rainfall measurements, similar to driving rain measurements, including adhesion water, evaporation, condensation, and splashing, are normally accounted in the product design. Therefore, it is reasonable to assume a measurement error specified by the manufacturer.

Wind-driven rain

The amount of rain impinged on the façade is measured using customized driving rain gauges. Driving rain gauges are not standardized instruments and they vary in size, shape, materials and recording mechanisms. The results from different driving rain gauges vary significantly (Van Mook, 2002). The duration, intensity, and type of rain event and the sampling frequency also affect the accuracy of the measurements. The errors associated with wind-driven rain measurement include adhesion water evaporation, condensation, splashing, and wind error. The error due to adhesion water evaporation is large for light rain (Blocken, 2004). The amount of wind-driven rain impinged on the collection area can only be measured after surface runoff occurs, when the accumulated wind-driven rain on the collector exceeds a threshold value. Below this threshold value, the rainwater impinged on the collector surface will evaporate. Above the threshold value, an approximately constant amount of water is adhered to the surface. When rain stops, this amount of adhered water will evaporate. The absolute error caused by adhesion water evaporation is significantly influenced by the amount of rain impinged on the surface.

To choose a material that has a better runoff property, laboratory tests were conducted to measure the maximum amount of adhesion water that can be held by different materials. In total, five materials were tested including regular glass sheet, polymethyl-methacrylate (PMMA, acrylic), aluminium, stainless steel, and polished stainless steel. A rectangular plate measuring 10" by 12" (25.40 cm by 30.48 cm) was made out of each material except for polished stainless steel, which has a dimension of 9" by 9" (22.86 cm by 22.86 cm). Each plate was subjected to 10 spray cycles using a spray bottle with adjustable nozzle. In each cycle, efforts were made to ensure consistency in terms of spraying from the

same distance and with approximately constant spray speed and droplet size. In each cycle, the sample was sprayed at four spots to cover the entire area until a significant amount of runoff occurred, then the plate was weighed and the mass of the adhesion water was calculated. Tap water was used for these experiments. The absolute measurement error due to adhesion is listed in Table 2.

Table 2. Absolute adhesion water on six vertically placed plates made of different materials.

	Glass	PMMA	Aluminium	Stainless steel	Polished stainless steel
Plate dimension (w×h) (mm)	254 × 304.8	254 × 304.8	254 × 304.8	254 × 304.8	228.6 × 228.6
Adhesion water (average) (mm or L/m²)	0.047	0.066	0.083	0.081	0.074
Adhesion water (stdev) (mm or L/m²)	0.0035	0.0034	0.0045	0.0059	0.0078

Glass has the best performance in terms of promoting water runoff; however, it is heavy and more difficult to fabricate and install. Polished stainless steel performs similarly to the acrylic sheet. With the consideration of durability, 14-gauge electro-plated stainless steel is chosen as the material for the driving rain gauge. A diamond shape of collector with a dimension of 9" by 9" (22.86 cm by 22.86 cm) is chosen. The edge of the collector is 25.4 mm high with an angle of 45° sloped inward to direct the runoff rainwater away from the gauge (Figure 2). The height of the edge is chosen to minimize the influence of the rim in deforming the wind flow and the trajectory of rain drops. The particular shape of the rain gauge allows the effective shedding of runoff rainwater from above away from the collector. To minimize the adhesion water, the connection tubing from the collector to the tipping bucket is made as short as possible (about 10 cm). The tipping bucket chosen for the driving rain gauge has a resolution of 2g/tip, which is equivalent to 0.038 mm per tip for the driving rain gauge with a collection area of 522.6 cm².

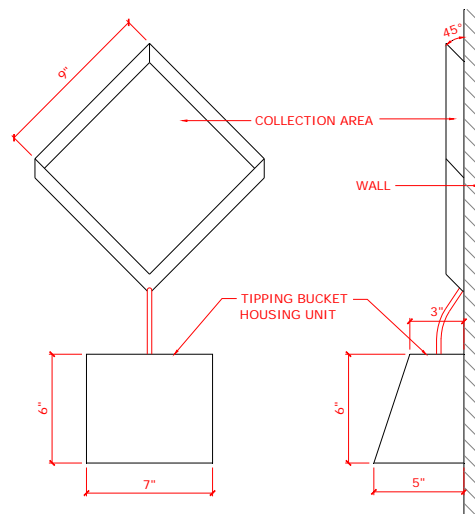


Figure 2. Sketch of the driving rain gauge.

The wind data (i.e., wind speed and wind direction) are gathered at 1 Hz sampling frequency and averaged over 1 minute. The horizontal and driving rain are collected at 5-minute intervals.





The locations of driving rain gauges installed on each building are shown in Appendix A. The data were downloaded through a telephone modem, and regular site visits were made to ensure the equipment working properly.





3 Data collection

Buildings 2, 3, 5, 6 and 7 were the first ones made ready for data collection. Buildings No. 1 and No. 8 are located on the BCIT Burnaby Campus and rain gauges were installed by December 2006. Building No. 4 belongs to the affordable housing and it took some time to receive approval for the installation of driving rain gauges, and, unfortunately, we did not get approval to install the weather station on the building. The wind and rain data recorded at the nearby air quality monitoring station by the Greater Vancouver Regional District will be used for analysis.

The first rain event started in mid October 2006, and data collection for the majority of buildings started in early November 2006. Data analysis reported here is based on the data collected until the end of July 2008. During the monitoring period, some instrument failures occurred including damage of the wind anemometer on Building No. 7 due to severe wind storms in the winter of 2007, the failure of a CR10X data logger used for Building No. 7 in the spring of 2008, and blockage of driving rain gauges. These incidences resulted in missing data for a short period of time. The raw data with incomplete information or data recorded when the driving rain gauge was blocked were discarded for the analysis. The data availability for each building is listed in Table 3.

Table 3. Summary of data collection.

Site	Geometry	No. of rain gauges	Meteorological parameters	Mast location	Data available	Remarks
Bldg. 1		2 (west) 2 (east) 1 (south)	<ul style="list-style-type: none"> • wind speed • wind direction • horizontal rainfall 	Weather data from Bldg. 8	November 23, 2006 to July 31, 2008	Rain gauges were inspected and cleaned in September 2007 and March 2008
Bldg. 2		3 (east) 1 (west) 1 (north) 1 (court yard)	<ul style="list-style-type: none"> • wind speed • wind direction • horizontal rainfall • relative humidity • temperature 	On top of the roof	November 2, 2006 to July 31, 2008	Rain gauges were inspected and cleaned in August 2007 and March 2008
Bldg. 3		5 (east) 1 (south)	<ul style="list-style-type: none"> • wind speed • wind direction • horizontal rainfall 	On top of the roof	October 27, 2006 to July 31, 2008	Rain gauges were inspected and cleaned in February and August 2007, and March 2008
Bldg. 4		3 (southwest) 1 (southeast)		No on-site weather data	February 21, 2007 to July 31, 2008	

Site	Geometry	No. of rain gauges	Meteorological parameters	Mast location	Data available	Remarks
Bldg. 5		5 (east) 1 (south)	<ul style="list-style-type: none"> wind speed wind direction horizontal rainfall 	<p>on top of a one-storey mechanical room located on the main roof (wind)</p> <p>on the main roof between the roof edge and the mechanical room (rain)</p>	January 1 2007 to July 31, 2008	Rain gauges were inspected and cleaned in February 2007 and March 2008
Bldg. 6		5 (east) 1 (north) 1 (west) 1 (south)	<ul style="list-style-type: none"> wind speed wind direction horizontal rainfall 	on top of a two-storey mechanical room located on the main roof (wind and rain)	December 19, 2006 to July 31, 2008	
Bldg. 7		4 (east) 2 (south, one with 3' (0.9 m) overhang, one with 1' (0.3 m) overhang)	<ul style="list-style-type: none"> wind speed wind direction horizontal rainfall 	<p>on top of a two-storey mechanical room located on the main roof (wind)</p> <p>on the main roof between the roof edge and the mechanical room (rain)</p>	December 14 2006 to July 31, 2008	<p>Wind anemometer was broken during the wind storm on Nov. 20 and fixed on Dec. 7, 2006.</p> <p>Rain gauges were inspected and cleaned in February 2007 and March 2008.</p> <p>CR10X data logger malfunction began on March 17 and was fixed on June 3, 2008.</p>
Bldg. 8		12 (east)	<ul style="list-style-type: none"> wind speed wind direction horizontal rainfall 	mast in front of the building (wind: 10 m above ground; rain: 2 m above ground)	December 15, 2006 to July 31, 2008	<p>Lost wind data for January and February due to malfunction of data logger.</p> <p>Two driving rain gauges discovered not working properly on Jan. 17, 2007 and they were fixed on Feb. 2, 2007.</p> <p>Rain gauges were inspected and cleaned in September 2007.</p>

4 Data Analysis

The data analyses include on-site wind and rain conditions, Driving Rain Index (DRI), and spatial distribution of wind-driven rain on wall surfaces. The effect of overhang is also discussed. The applicability of using an empirical method to estimate driving rain on specific walls is examined.

4.1. On-site wind and rain conditions

The analyses of on-site wind and rain conditions include the prevailing wind direction during rain hours and all hours (Figure 3), wind speed distribution during rain hours and all hours (Figure 4), seasonal variation of wind speed, and rainfall intensity distribution.

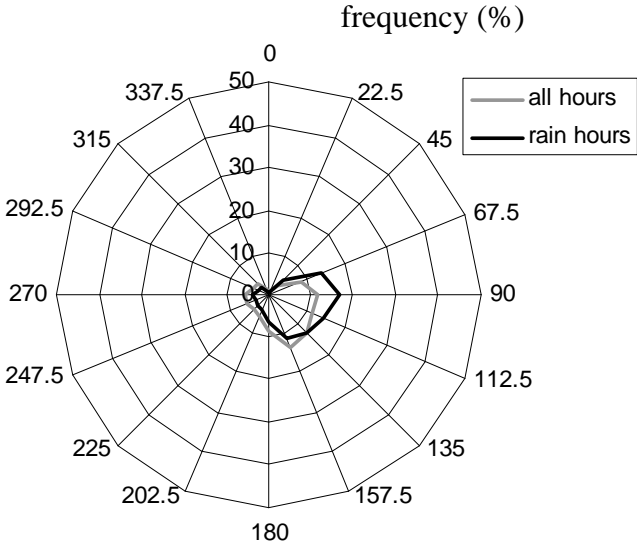
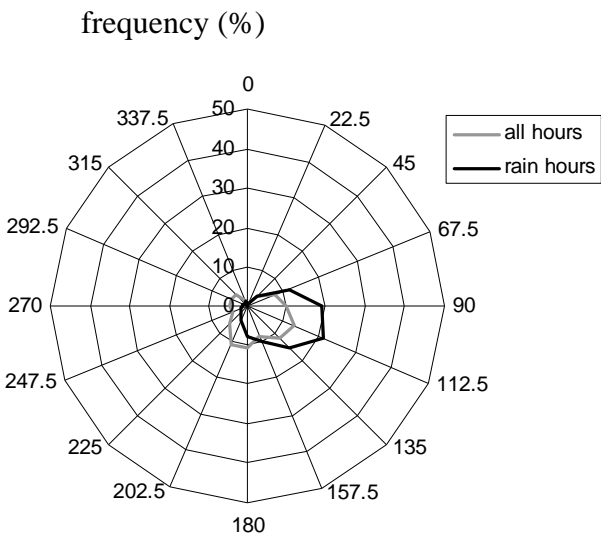


Figure 3a. Prevailing wind direction for Buildings 1 & 8. Figure 3b. Prevailing wind direction for Building 2.

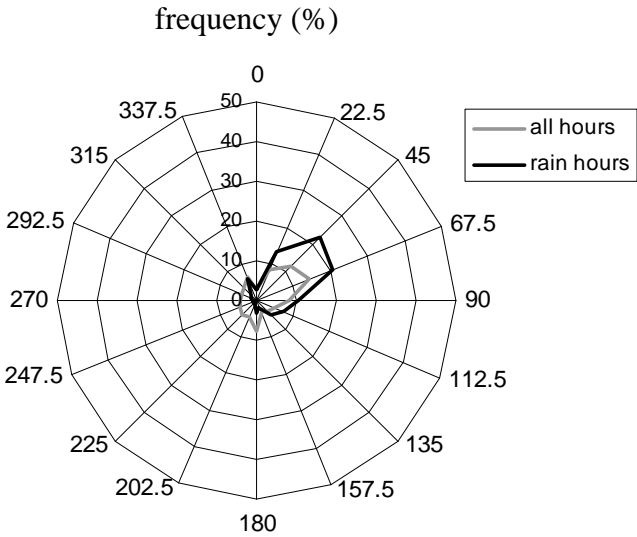
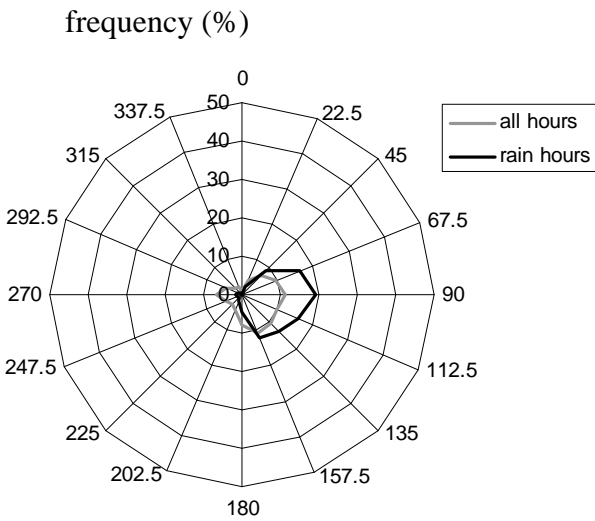


Figure 3c. Prevailing wind direction for Building 3. Figure 3d. Prevailing wind direction for Building 5.

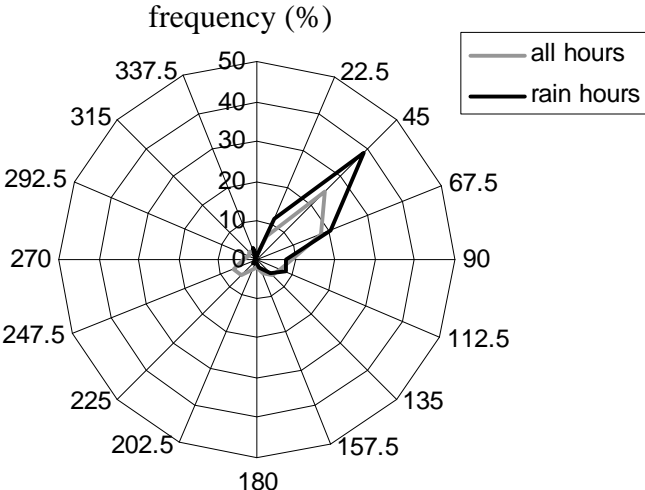
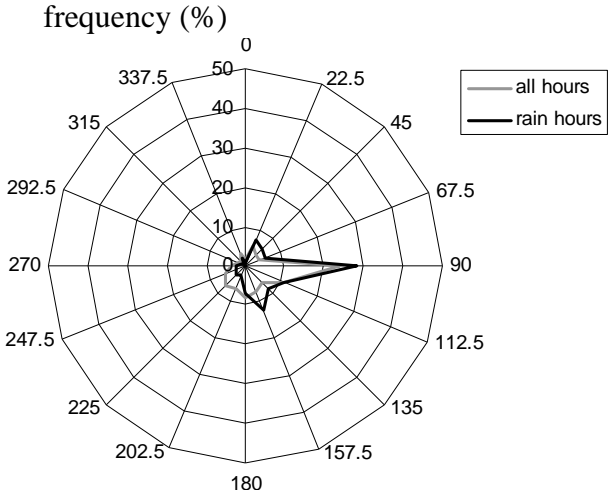


Figure 3e. Prevailing wind direction for Building 6. Figure 3f. Prevailing wind direction for Building 7.

The prevailing wind direction is from the east-south-east for Building No. 1, and the east with a slightly lower frequency of wind from the east-north-east for Buildings No. 2 and 3 during rain hours. The wind rose shape is more widely dispersed between the east-north-east and south-south-east. For Building No. 5 (medium height building) and No. 7 (high-rise), the prevailing wind direction is more distinct from the northeast. For the high-rise building in Burnaby (Building 6), the prevailing wind direction is from the east with a second highest frequency of wind from the south-south-east. In general, there is only a slight difference in the statistics of wind direction between all hours and rain hours. Seasonal wind roses were generated as well. There is no significant variation in prevailing wind direction among different seasons.

The wind speed is measured at about 10 m above ground for the low-rise buildings. The wind speed distribution is very similar for Buildings No. 8 (BCIT Burnaby Campus) and No. 2 (Wallace building located near Jericho Beach, within 1 km of direct water exposure). The predominant wind speed is less than 2 m/s. The wind speed recorded for Building No. 3, a three-storey low-rise building, is higher with the predominant wind speed in the range of 2–4m/s, probably due to the more open building site and its local topography. The wind speed distribution is similar for the two high-rise buildings. With the increase in building height, the wind speed increases. However, the predominant wind speed is within the range of 2–6 m/s. In general, the average wind speed is slightly higher during rain hours than during all hours.

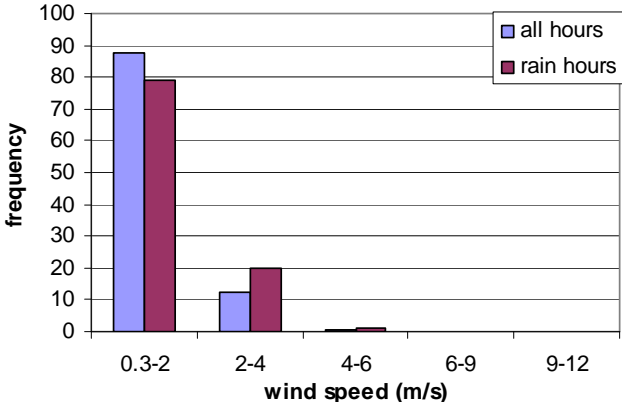
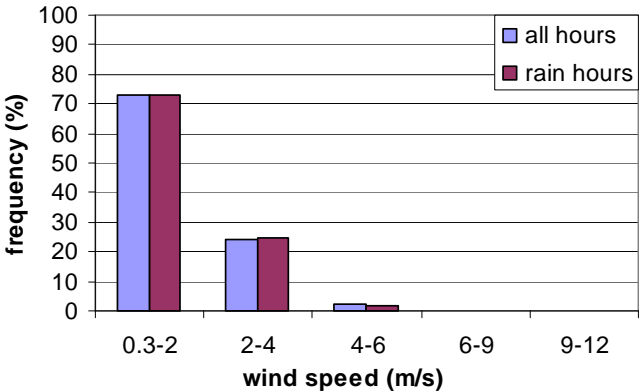


Figure 4a. Wind speed distribution for Buildings 1 & 8. Figure 4b. Wind speed distribution for Building 2.

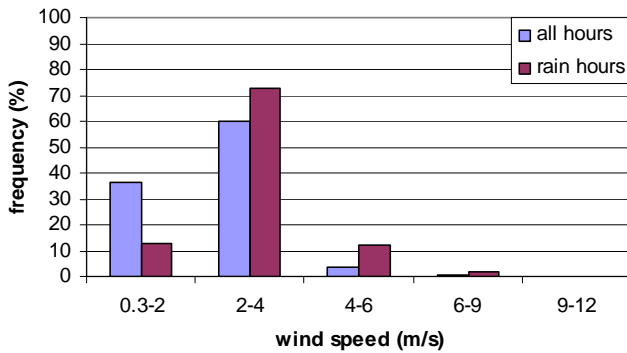


Figure 4c. Wind speed distribution for Building 3.

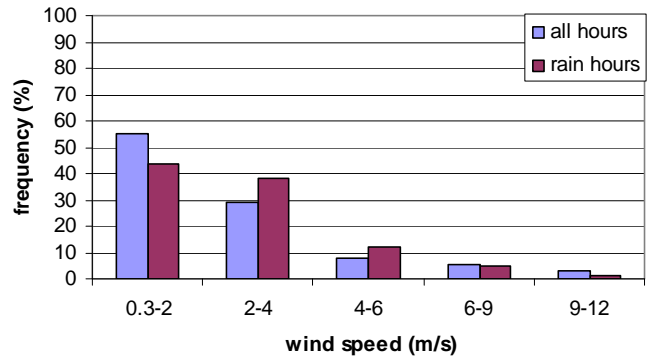


Figure 4d. Wind speed distribution for Building 5.

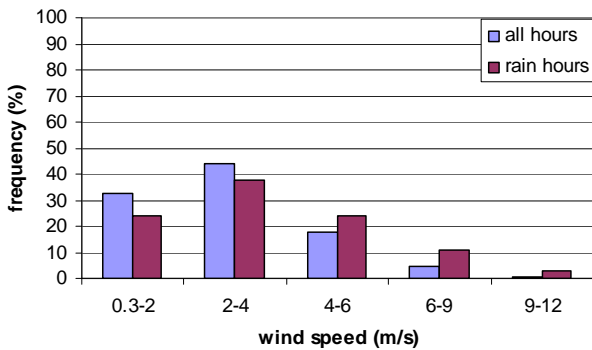


Figure 4e. Wind speed distribution for Building 6.

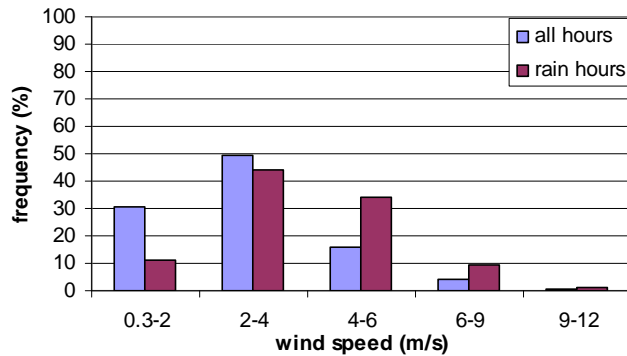


Figure 4f. Wind speed distribution for Building 7.

The monthly average and maximum wind speed on each building site is listed in Table 4. The BCIT Burnaby Campus (Buildings 1 and 8) and Building 2 sites experience lower wind speed. The monthly average wind speed during rain for these two sites is within 1.5 m/s. Building No. 3, a three-storey building, has wind conditions similar to Building No. 5, the medium height building with an average monthly wind speed within 2.2 to 3.0 m/s. The wind speed on top of the high-rise buildings is slightly higher with a monthly average wind speed in the range of 3.0 to 4.0 m/s. The maximum wind speed recorded during rain hours is lower than that during all hours.

Table 4. Wind speed recorded for each building site.

Building sites	Height of wind measurements (m)	Wind speed as measured (m/s)				Equivalent wind speed at 10 m above the ground (m/s)*	
		Monthly average (m/s)		Maximum (m/s)		All hours	Rain hours
		All hours	Rain hours	All hours	Rain hours		
Buildings 1 & 8	10.0	1.56	1.50	13.29	7.84	1.56	1.50
Building 2	11.6	1.19	1.31	12.98	8.12	1.15	1.26
Building 3	11.3	2.42	2.86	10.42	10.17	2.35	2.77
Building 5	25.3	2.20	2.60	22.34	15.68	1.75	2.06
Building 6	51.2	2.99	3.57	19.71	19.71	1.99	2.37
Building 7	41.2	2.93	3.73	16.36	14.19	2.06	2.62

* An exponent of $\alpha=0.25$ is used to convert the wind speed measured at height h to 10 m above ground for the relatively open urban area.

The seasonal variations of average wind speed for each building site over the monitoring period are listed in Table 5. The average wind speed varies slightly over seasons. In general, the wind speed during the winter season is the highest followed by the spring, fall and summer for all hours. The wind speed during the winter is also the highest during rain hours, followed by the fall, spring, and summer.

Table 5. Seasonal variations of wind speed recorded for each building site.

Building sites	Wind speed as measured (m/s)											
	Winter 2006		Spring 2007		Summer 2007		Fall 2007		Winter 2008		Spring 2008	
	all hours	rain hours	all hours	rain hours	all hours	rain hours	all hours	rain hours	all hours	rain hours	all hours	rain hours
1 & 8			1.62	1.54	1.56	1.24	1.39	1.62	1.48	1.52	1.69	1.52
2	1.21	1.53	1.30	1.22	1.13	1.03	1.04	1.38	1.20	1.54	1.20	1.14
3	2.56	3.22	2.45	2.71	2.28	2.45	2.28	2.96	2.46	3.18	2.42	2.58
5	2.35	3.32	2.29	2.68	2.06	2.16	1.85	2.77	2.28	2.73	2.26	2.30
6	3.11	4.23	3.02	3.56	2.78	3.13	2.85	3.96	3.25	4.08	2.83	2.85
7	3.10	4.14	3.04	3.59	2.77	3.11	2.76	3.62	3.08	4.01	2.77	3.35

For the purpose of comparison, the total amount of rainfall measured and the average hourly rainfall intensity for each building site from January to December 2007 are listed in Table 6.

Table 6. Total amount of rainfall and the average hourly rainfall intensity measured from January to December 2007 for each building site.

Building sites	Rainfall amount (mm)	Average hourly rainfall intensity (mm/hr)
Buildings 1 & 8	1726.5	2.13
Building 2	1476.1	1.95
Building 3	1611.6	2.04
Building 5	1807.4	2.27
Building 6	1515.2	1.81
Building 7	1840.9	2.13

The average hourly rainfall intensity is about 2 mm/hr for all sites. The total amount of rainfall recorded varies slightly among the building sites. Building 2 receives the lowest amount of rainfall and Building No. 7 receives the highest.

4.2. Airfield Driving Rain Index

The rate at which driving rain is incident on an unobstructed imaginary wall surface can be calculated from the rainfall rate and wind speed using empirical relationships between rainfall rate and drop size distribution (Laws & Parsons, 1943) and drop size and terminal velocity (Best, 1950), as expressed in Equation (1).

$$R_{\text{airfield}} = \frac{2}{9} \cdot U \cdot R_h^{8/9} \cos(\theta - 90^\circ) \quad (1)$$

Where, U is the wind speed in m/s against the wall;
 R_h is the horizontal rainfall in mm/hr; and
 θ is the wind direction.

The driving rain in the airfield is a relative indicator of the severity of a specific wall orientation to the wind-driven rain exposure, but not the actual amount of driving rain deposited on the wall surfaces. The actual amount of wind-driven rain received by a specific wall surface at a specific location is influenced by the airflow along building surfaces, which is a result of the interaction between the wind and the building. The effect of building geometry and details are normally accounted for by a correction factor. For example, the British Standard BS-8104 (1992) introduces a wall factor, which is defined as the ratio of the quantity of rainwater falling on a wall and the quantity falling on an equivalent unobstructed surface. It takes into account the influence of airflow around the building and local sheltering such as eaves and sills, etc. Straube and Burnett (2000) introduced a similar term called the Rain Deposition Factor to account for the effect of building shape and size on rain deposition.

The Driving Rain Index at roof-line height is calculated for eight wall orientations using Equation 2 for each monitored building.

$$DRI = \sum \frac{2}{9} \cdot U \cdot R_h^{8/9} \cos(\theta - 90^\circ) \quad (2)$$

Five-minute data collections are used for the calculation. The recorded 1-minute wind data (wind speed and wind direction) are averaged over 5-minute intervals. The summation is taken over all 5-minute intervals when $\cos(\theta-90)$ is positive, i.e., all those occasions when the wind is blowing against the wall.

The wind speed measured at the mast is converted to a wind speed at the roof-line height. The standard approach used to correct wind speed with height is provided in the National Building Code of Canada (NBCC 1996). The wind speed at any height, $U(h)$, can be found from:

$$U(h) = U_{10} \cdot (h/10)^\alpha \quad (3)$$

Where, U_{10} is the standard wind speed at 10 m above grade, normally reported by weather stations (m/s); and
 h is the height above grade (h).

The recommended exponent $\alpha=0.25$ for a suburban terrain is used since most of the building sites are located in a relatively open urban area.

Figure 5 shows the airfield driving rain on walls with eight different orientations for the period of measurements, and the actual amount of wind-driven rain measured on a location close to the roof line is also shown. The difference between the airfield DRI and the actual amount of driving rain (DR) measured on the façade indicates the significant influence of building geometry and its design detail. As shown in Figure 5a and 5c, the difference between driving rain measured on the wall surface and the airfield Driving Rain Index is significantly smaller than that for other buildings due to the lack of overhang protection.

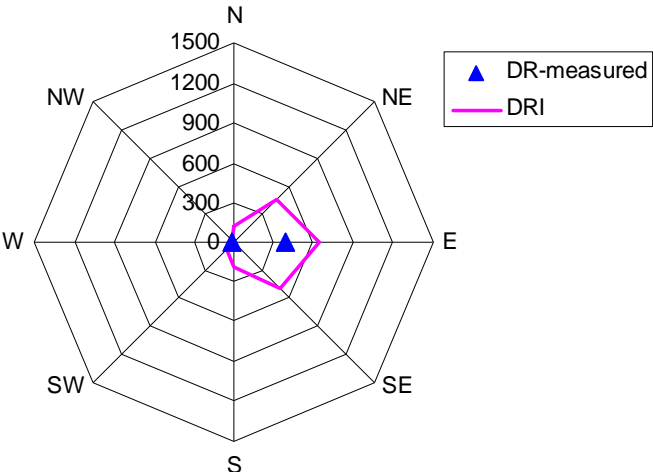


Figure 5a. Airfield Driving Rain Index and measured driving rain impinged on the east and west walls of Building 2 for the period of November 2006 to July 2008 (unit in mm).

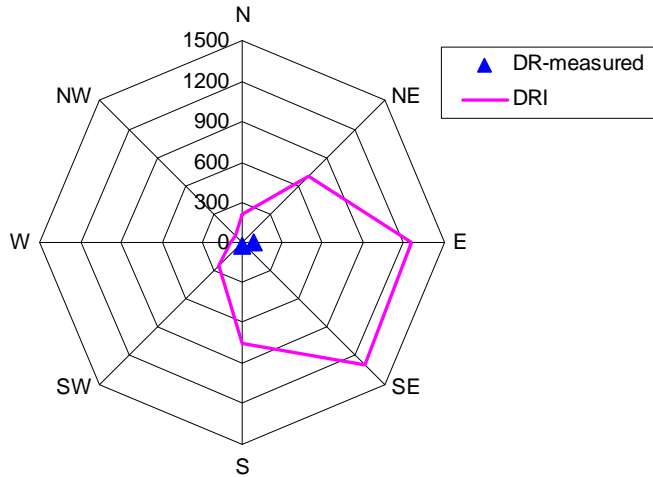


Figure 5b. Airfield Driving Rain Index and measured driving rain impinged on the east and south walls of Building 3 for the period of November 2006 to July 2008 (unit in mm).

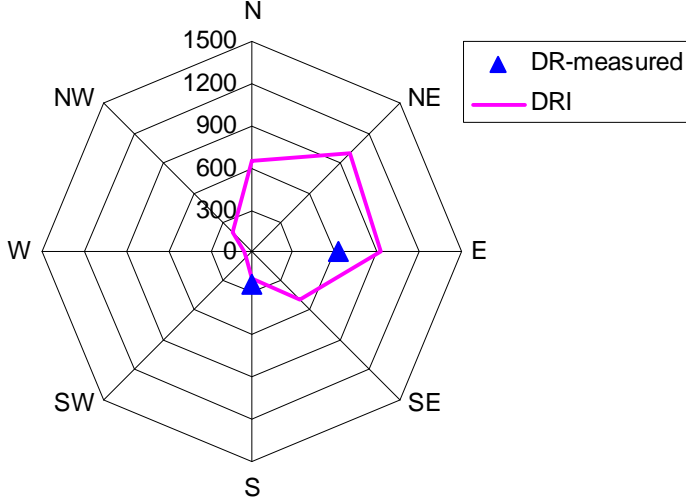


Figure 5c. Airfield Driving Rain Index and measured driving rain impinged on the east and south walls of Building 5 for the period of January 2007 to July 2008 (unit in mm).

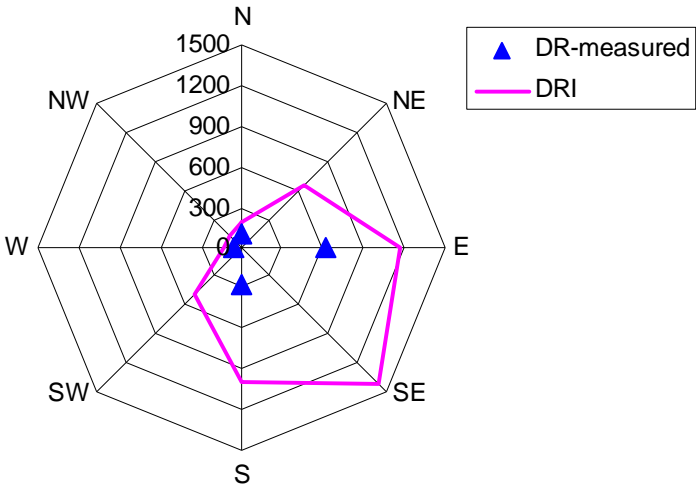


Figure 5d. Airfield Driving Rain Index and measured driving rain impinged on the four orientations of Building 6 for the period of December 2006 to July 2008 (unit in mm).

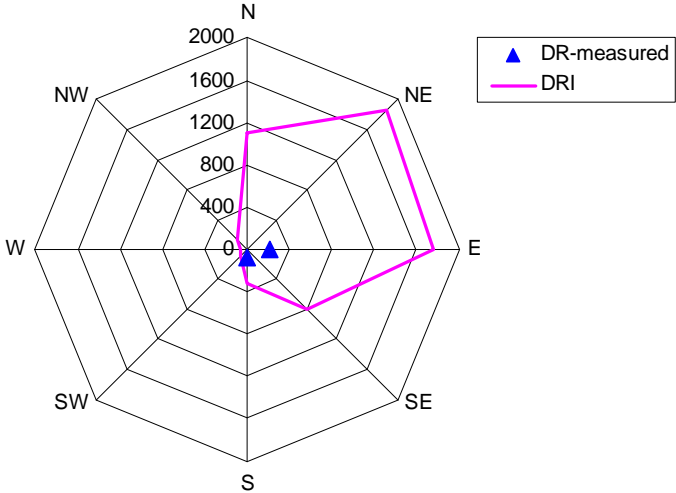


Figure 5e. Airfield Driving Rain Index and measured driving rain impinged on the east and south walls of Building 7 for the period of December 2006 to July 2008 excluding March, April, and May 2008 due to the failure of the data logger (unit in mm).

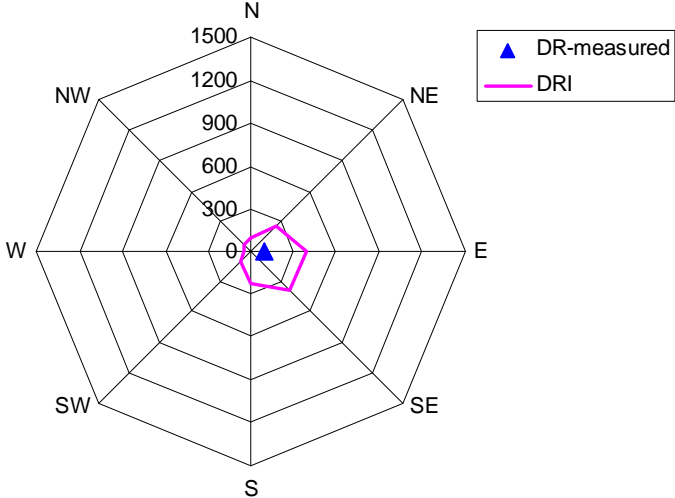


Figure 5f. Airfield Driving Rain Index and measured driving rain impinged on the east wall of Building 8 for the period of March 2007 to July 2008 (unit in mm).

The analysis of the airfield Driving Rain Index indicates the potential wetting on each orientation. To compare the wind-driven rain exposure of these six building sites, the airfield Driving Rain Index calculated during the same monitoring period is listed in Table 7. All buildings are oriented cardinally; therefore, available driving rain measured on these cardinal orientations is listed as well. Among the four cardinal directions, the east-facing walls have the most severe wind-driven rain exposure for all buildings monitored, and the south-facing walls have the second most severe wind-driven rain exposure for most buildings, except for Buildings 5 and 7. For Building 5 and Building 7, the north-facing walls have the second-worst wind-driven rain exposure. Given that the north-facing walls receive the least amount of solar radiation, i.e., the least drying potential, north-facing walls may be more prone to moisture damage.

By comparing the actual amount of driving rain measured on the walls to the airfield DRI, it shows that building geometry and design details have a significant influence on a building's wind-driven rain exposure. For example, Building 7 has the highest Driving Rain Index; however, the measured driving rain is only one-third of the amount measured on Building 6, which has a smaller Driving Rain Index. The presence of a 3' (0.9 m) overhang on top of this high-rise building significantly reduced the wind-driven rain exposure. The similar trend is observed for Building 3. Building 3 has as much as double the amount of Driving Rain Index as Building 2; however, the driving rain measured is only about 27% of the amount measured on Building 2 because of the presence of a 1' (0.3 m) overhang on Building 3. The effect of overhang is discussed further in section 4.4.

Table 7. Airfield Driving Rain Index analysis for the six building sites for the period of January to December 2007.

Building sites	Worst orientation	Airfield DRI (mm)								Measured Driving Rain (mm)			
		N	NE	E	SE	S	SW	W	NW	N	E	S	W
Bldg. 2	E	70.2	259.5	372.0	290.1	112.1	40.1	19.7	11.4		207.0		7.0
Bldg. 3	SE	117.8	371.6	697.3	732.2	451.7	143.4	42.0	33.7		54.9	21.5	
Bldg. 5	NE	441.5	740.4	739.1	413.3	159.6	41.4	32.6	113.0		579.9	192.5	
Bldg. 6	SE	129.7	483.8	889.3	1089.7	751.7	346.3	72.8	72.5	69.9	474.4	234.5	37.8
Bldg. 7	NE	855.7	1411.9	1358.3	633.3	264.5	61.7	39.9	119.0		167.2	73.1	
Bldg. 8*	SE	70.7	156.3	240.9	260.0	158.4	66.8	26.6	46.4		100.2		

* Data shown for Building 8 is for the period from March to December 2007 because of the failure of wind measurements for January and February, 2007.

4.3. Spatial distribution of wind-driven rain on the façade

To indicate the spatial distribution of wind-driven rain on the façade, both the catch ratio and wall factors are used. The catch ratio is defined as the total amount of driving rain collected on the wall surface divided by the total amount of horizontal rainfall over the same time period (Equation 4).

$$\eta = \frac{R_{wdr}}{R_h} \quad (4)$$

As outlined in the British Standard BS-8104 (1992), the actual wind-driven rain impinged on building surfaces can be quantified using Equation (5) to convert the airfield indices to wall indices:

$$R_{wdr} = R_{airfield} \cdot R \cdot T \cdot O \cdot W \quad (5)$$

Where, R is the terrain roughness factor that takes into account the variability of the mean wind speed at the site due to the height above the ground and the upstream roughness of the terrain;

T is the topography factor that accounts for the increase of the mean wind speed over isolated hills and escarpments;

O is the obstruction factor that takes into account the shelter by the nearest obstacle of similar dimensions to the wall; and

W is the wall factor that takes into account the variation of wind-driven rain over the surface of the wall.

Since the on-site wind and rain data are available, in the analysis the factors R , T , and O are deemed as 1.0. Therefore, the wall factor is calculated as the ratio of the airfield DRI to the actual amount of driving rain measured at a specific location (Equation 6).

$$W = \frac{R_{wdr}}{R_{airfield}} = \frac{R_{wdr}}{\frac{2}{9} R_h^{8/9} U \cos(\theta - 90)} \quad (6)$$

The catch ratio and wall factors for each specific location measured are listed in Appendix A. As a summary, the wall factors based on the measurements for the east façades are listed in Table 8. In the meantime, the available literature data for similar building geometries are also presented in Table 8.

For the two-storey building with pitched roof and overhang (Building 1), the wall factor at the middle height of the building is about 0.16, which is lower than the literature data from the British Standard and Straube (2006). For the location underneath the overhang, the measured result is much lower than the literature data.

For the three-storey building with low-sloped roof and 1' (0.3 m) overhang (Building 3), the wall factors are much smaller than reported from the British Standard for a two-storey flat roof with no-overhang building because of the protection provided by the overhang and also the specific wind and rain characteristics.

For the 16-storey high-rise building without overhang (Building 6), at the top east corner (0.6m below the roof line), a wall factor of about 0.5 is estimated. This is the same as recommended by the British Standard and slightly lower than the values recommended by Blocken (2004). For the remainder of the building, the wall factors vary from 0.084 to 0.326, observed for the portion from the 1/2 height of the building up to 8' below the roofline. Straube (2006) recommended a much larger value for the high-rise building. The discrepancy could be attributed to the mild wind in the Vancouver region.

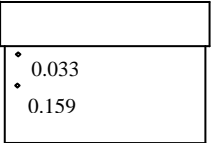
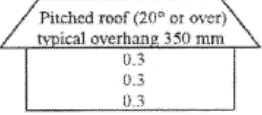
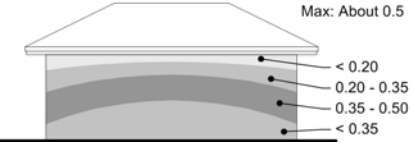
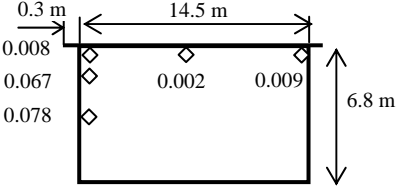
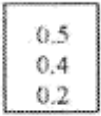
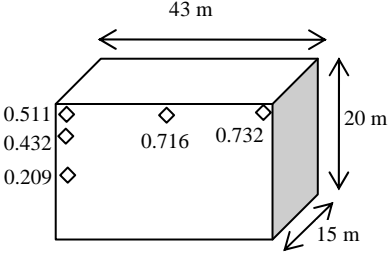
For the long low aspect ratio building with a small overhang (Building 8), the measured values are smaller at the top of the building than recommended by Straube (2006) and Blocken (2004), probably due to the presence of the overhang and again the particular wind and rain conditions. The slightly lower wall factors at the corner compared to the locations in the middle are the result of wind approaching the wall surface at an angle from the southeast for most of the time. A similar wetting pattern is also observed on Building 5. As listed in Table 8, the wall factor is the highest at the north corner (0.732) followed by the wall factor at the center (0.716) and at the south corner (0.511) due to a prevailing wind direction from the northeast for this building site. Both wind-tunnel measurements (Inculet and Surry, 1994) and CFD simulations (Blocken and Carmeliet, 2004) have observed the

similar distribution. More rain is deposited on the upwind façade than on the downwind façade when wind approaches the building at an angle.

It should be noted that the values recommended by the British Standard (BSI, 1992) and Straube (2006) are based on long-term field measurements and do not account for specific wind and rain conditions. Values recommended by Blocken (2004) are generated through a validated CFD model and are specific to wind and rain conditions. The values reported in Table 8 are average values estimated for all wind and rain events during the monitoring period. In general, the wall factors obtained through field measurements are similar or smaller than reported in literature probably because of the mild wind and rain conditions and the presence of overhang.

The detailed CFD simulation by Blocken (2004) showed that the spatial distribution of wind-driven rain on the building façade is influenced by the specific wind and rain conditions, i.e., wind speed, rainfall intensity, and wind direction. The catch ratio increases approximately linearly with wind speed. There is generally a steep increase of the catch ratio with increasing horizontal rainfall intensity for light rain with rainfall intensity below 1 mm/hr. When the rainfall intensity is greater than 1 mm/hr, its increase has no impact on the catch ratio. Wind speed has more significant influence than the rainfall intensity on the amount of wind-driven rain deposited on the building façade. The increase of wind angle results in the reduction of rain deposition on the wall surface. The on-site weather data reported in section 4.1 show slightly seasonal variations in wind speed. The typical rainy season in the coastal region of BC is from late fall to early spring. The wind speed is slightly higher during these seasons, and so is the amount of driving rain deposited on building façades. The seasonal variation of spatial distribution of wind-driven rain (catch ratio) is also calculated for each building. Table 9 shows the results for Building No. 6 as an example, and the detailed catch ratio values for each building are listed in Appendix A. The monitoring period includes two winter and two spring seasons and one summer and one fall season. The catch ratios for the winter and spring seasons listed in Table 9 are the average over the two winter and two spring seasons monitored. In general, the catch ratio during the winter is the highest, followed by the fall or spring, and the catch ratio during the summer is the lowest.

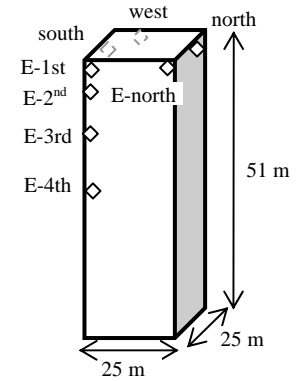
Table 8. Comparison of the spatial distribution of wind-driven rain (wall factors) determined from the field measurements to values reported in literature.

	Field measurements	BS1804 (1992)	Straube (2006)	Blocken (2004) (wind speed $U_{10}=2\text{m/s}$, $R_h=2\text{mm/hr}$)
Building 1: 2-storey with 1' overhang (pitched roof)				
Building 3: 3-storey with 1' overhang (low-sloped roof)				
Building 5: 6-storey building without overhang				

	Field measurements	BS1804 (1992)	Straube (2006)	Blocken (2004) (wind speed $U_{10}=2\text{m/s}$, $R_h=2\text{mm/hr}$)
Building 6: 16-storey high-rise without overhang		0.5 for the top 2.5 m 0.2 for remainder	<p>Tall Building ($>10\text{m}$) $H/W \gg 1$</p>	
Building 7: 12-storey high-rise with 3' overhang				
Building 8: low aspect ratio building with 1/2' overhang			<p>Low-rise Building $H/W \ll 1$</p>	

Table 9. Seasonal variation of spatial distribution of wind-driven rain on Building No. 6

Driving rain gauge location	Catch Ratio				
	Winter	Spring	Summer	Fall	Average over the entire monitoring period
E-1 st	0.368	0.246	0.212	0.287	0.304
E-2 nd	0.263	0.131	0.114	0.181	0.184
E-3 rd	0.112	0.057	0.047	0.061	0.081
E-4 th	0.060	0.031	0.033	0.044	0.043
E-north	0.215	0.133	0.110	0.177	0.175
South	0.158	0.126	0.088	0.183	0.153
West	0.029	0.034	0.068	0.038	0.033
North	0.058	0.038	0.032	0.076	0.051



4.4. Effect of overhang

The field survey of building envelopes indicates that the presence of an overhang helps reduce the level of moisture damage (CMHC, 1996). The previous measurements we took on the campus building (Bldg. 8) showed that a 6" overhang may reduce the wind-driven rain exposure for a long low-aspect building by two to five times depending on the wind and rain characteristics (Ge and Krpan, 2007). The newly collected data help to analyze the protection provided by the overhang for more building geometries. Figure 6 shows the highest catch ratio on the east façade of each monitored building. The catch ratios range from 0.18 for a low-rise to 0.37 for the medium-height and 0.30 for the high-rise building without overhang, while, for the three buildings with overhang, the catch ratio is less than 0.05 for low-rise buildings and 0.09 for a high-rise building.

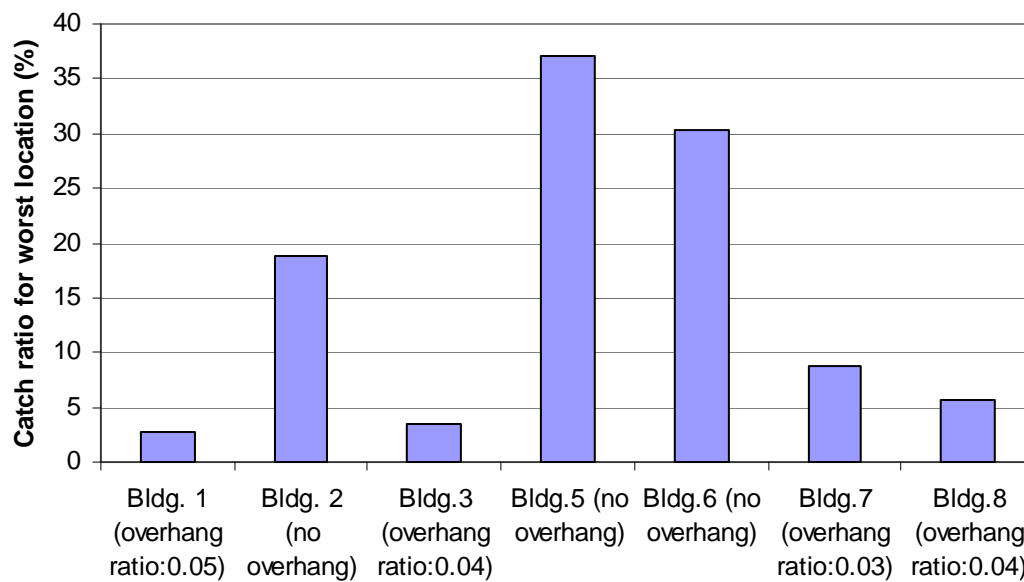


Figure 6. Effect of overhang by comparing the highest catch ratio for the east wall on each building.

To estimate the total protection provided by the overhang for the whole wall surface, the area-weighted catch ratio is calculated for Buildings 1, 2, 3, 6, 7 and 8. An overhang protection factor is defined as the ratio of the average catch ratio of the reference building to the average catch ratio of the test building

(equation 7). For low-rise buildings, Building 2 (without overhang) serves as the reference building, and for high-rise buildings, Building 6 (without overhang) serves as the reference building. As shown in Appendix A, rain gauges on the east façade were installed at 2' and 8' below roof line, ¼ height and/or ½ height of the building. For buildings having rain gauges within the first ¼ height, at ¼ and ½ height, it is assumed that the first ¼ wall surface receives an amount of driving rain as measured by rain gauges within the upper ¼ height, the second ¼ wall surface receives an amount of driving rain as measured by the rain gauge located at the ¼ height of the building, and the remainder ½ wall surface receives an amount of driving rain as measured by the rain gauge located at the ½ height of the building (equation 8). For buildings with rain gauges located only at the upper ¼ height and ¼ or ½ height of the building, it is assumed that the first ¼ of the wall surface receives an amount of driving rain as measured by the rain gauges within the upper ¼ height and the remaining ¾ of the area receives an amount of driving rain as measured by the rain gauge located at ¼ or ½ height of the building (equation 9).

$$\text{Overhang protection factor} = \frac{\eta_{test}}{\eta_{reference}} \quad (7)$$

$$\text{Average-weighted catch ratio } \eta_{test} = 1/4\eta_{top} + 1/4\eta_{middle} + 1/2\eta_{bottom} \quad (8)$$

or

$$\text{Average-weighted catch ratio } \eta_{test} = 1/4\eta_{top} + 3/4\eta_{middle} \quad (9)$$

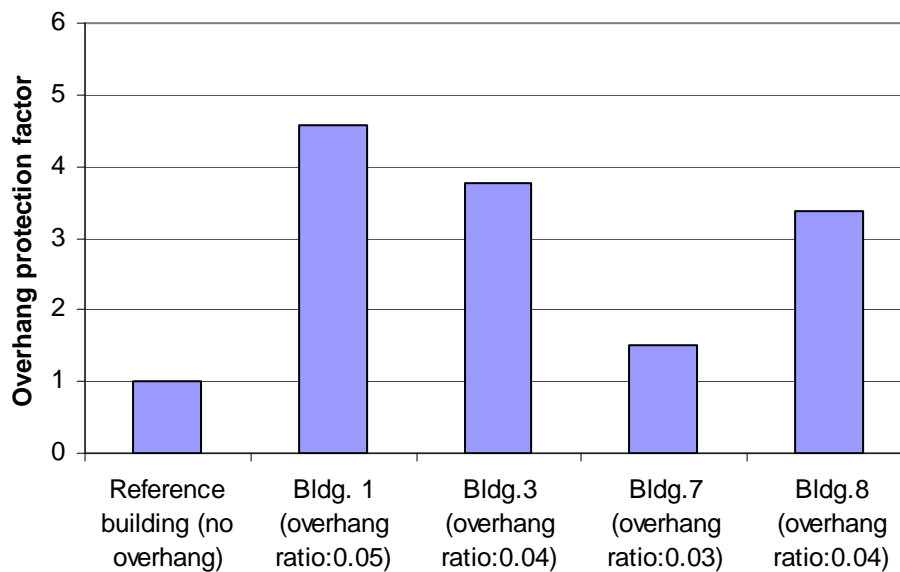


Figure 7. Protection provided by the overhang for four buildings.

The overhang ratio, the width of the overhang divided by the wall height, is almost the same for all four buildings. As shown in Figure 7, the presence of an overhang can reduce the amount of wind-driven rain for low-rise buildings about four times, and one and a half times for the high-rise building No. 7. This is only a rough estimation since these buildings do not have exactly the same geometry and are located in different microclimates, although site analysis indicates that these sites have similar wind and rain conditions.

Another interesting observation is the protection area provided by the overhang. For buildings without overhang or other protection, the wetting increases with the height of the building, as shown in Figure 8a. For the high-rise building with a 3' (0.9 m) overhang, the wetting is significantly reduced for the location right underneath the overhang (Figure 8b). The catch ratio for the second location (about 2.5 m below the roof line) is slightly higher than the third location (1/4 of the total building height), which indicates that this location is still partially protected by the roof overhang, and the protection line lies between 2.5 m and the 1/4 building height, i.e., 10 m. The catch ratio at 1/4 of the building height is similar to that for the high-rise building without any protection, which indicates that the protection provided by a roof overhang diminishes below this point. Incullet and Surry (1994) did a wind-tunnel measurement to evaluate the effect of overhang and cornice, and they found that for a 1 m overhang the protection area is about 0.75 m below the roof line for a similar 40 m high building when tested under a wind speed of 12 m/s. The observed much larger protection area provided by the overhang may be attributed to the much lower wind speed.

For low-rise Building 3, the protection area extends beyond the 1/2 height of the building as indicated by a higher catch ratio at the third location than that at the second location (Figure 8c).

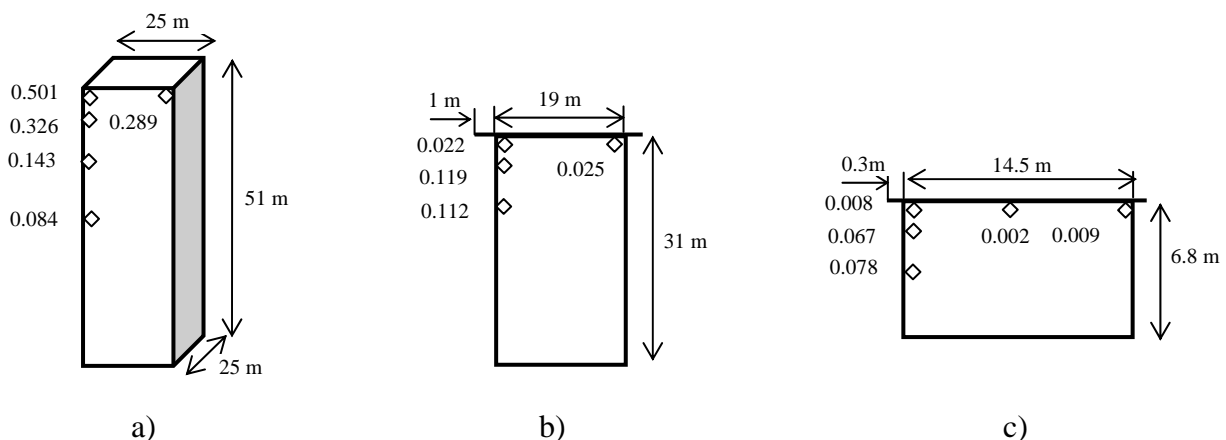


Figure 8. Effect of overhang by comparing the spatial distribution of catch ratios among Buildings 6, 7, and 3.

4.5. Assessment of wind-driven rain on wall surfaces using empirical correlations

As described in section 4.3, the actual wind-driven rain impinging on the building façade can be estimated using semi-empirical methods such as the procedure prescribed by the British Standard BS-8104. This procedure involves converting the airfield indices, which are calculated based on the weather data, i.e., wind speed, wind direction, and rainfall intensity collected from meteorological stations, to wall indices by introducing four correction factors. This method was developed based on a long series of measurements of driving rain on buildings in a wide range of locations within the UK. As such, the method is applicable to climates similar to the UK, and direct measurement of wind-driven rain on building façades is recommended in mountainous areas. The wind and rain conditions can vary significantly in the southern BC region, even over a small regional scale due to the influence of the local topography and other factors such as the ocean. Although the procedure prescribed by BS-8104 is not recommended for the mountainous areas, it is not always practical to have direct measurements of wind-driven rain on specific buildings when such information is required for the building envelope design. The availability of direct measurements on a range of buildings generated through this project presents a good opportunity to evaluate the applicability of this semi-empirical method in this particular

climate. The Lower Fraser Valley of BC contains the ambient air quality monitoring network of the Greater Vancouver Regional District. Many of the stations in this network measure wind speed and direction as well as precipitation. One year’s weather data from these stations (Oct. 1, 2006 to September 30, 2007) are requested. By examining the completeness of wind and rain information and the proximity of its location to the monitored buildings, three stations are chosen (Table 10).

Table 10. GVRD weather stations.

Station information	In the proximity of monitored buildings
Vancouver Airport station, T31 Address: 3153 Templeton St., Richmond Latitude: 49° 11' 11"; Longitude: 123° 09' 08"; Elevation: <15 m	
Kitsilano Station, T2 Address: 2550 W. 10 th Ave., Vancouver Latitude: 49° 15' 42"; Longitude: 123° 09' 48"; Elevation: 63 m	Building 2
Burnaby South station, T18 Address: 5455 Rumble St., Burnaby Latitude: 49° 12' 55"; Longitude: 122° 59' 08"; Elevation: 145 m	Buildings 3, 6

The error in calculating wind-driven rain deposition on the building façade using wind and rain data from weather stations can be estimated by the error in calculating the airfield Driving Rain Index using the data from weather stations (Equation 10). The derivation of Equation 10 is shown as follows:

As per Equations 1 and 5, the amount of wind-driven rain deposited on the building façade is:

$$R_{wdr-cal} = R_{airfield-station} \cdot R \cdot T \cdot O \cdot W$$

$R_{airfield-station}$ is Driving Rain Index calculated using wind and rain data from the weather station;

Since no building is located on a hill or escarpment, the local topography factor R for all buildings monitored is 1.0. All of the five buildings are located in relatively exposed areas; therefore, obstruction factor O can be considered as 1.0. The wall factor, W, is calculated using the direct driving rain measurement and the airfield Driving Rain Index calculated using on-site wind and rain data, as indicated in Equation 6; therefore,

$$R_{wdr-cal} = R_{airfield-station} \cdot T \cdot \frac{R_{wdr-measured}}{R_{airfield-onsite}}$$

Then,

$$\frac{R_{wdr-cal}}{R_{wdr-measured}} = \frac{R_{airfield-station}}{R_{airfield-onsite}} \cdot T, \text{ and}$$

$$error(R_{wdr-cal}) = error(R_{airfield-station}) \cdot T \tag{10}$$

Table 11 lists the errors in estimating wind-driven rain on five monitored buildings using weather data from the Vancouver International Airport station for the monitoring period from January 1 to September 30, 2007. The terrain roughness factor T is 0.75 according to the British Standard BS-8104 for the category of land with closely spaced obstructions, such as buildings and trees. The comparison

between the airfield Driving Rain Index calculated using weather data collected on site and from the airport station for the five buildings is shown in Figure 9.

Table 11. Errors in estimating wind-driven rain on five monitored buildings using weather data from the Vancouver International airport station for the monitoring period from January 1 to September 30, 2007.

Orientation	DRI- Airport station	DRI- Bldg. 2	error (%)	DRI- Bldg. 3	error (%)	DRI- Bldg. 5	error (%)	DRI- Bldg. 6	error (%)	DRI- Bldg. 7	error (%)
N	37.7	50.4	-25.1	77.6	-51.3	248.9	-84.8	65.6	-42.5	423.8	-91.1
E	352.3	252.3	39.6	524.0	-32.8	440.1	-19.9	438.7	-19.7	652.5	-46.0
S	126.6	80.1	58.1	350.0	-63.8	106.9	18.5	314.5	-59.7	126.9	-0.2
W	20.0	15.0	33.7	31.6	-36.8	23.1	-13.5	27.0	-26.0	18.9	5.8
Sum of error square			6713.2		9137.5		8117.3		6432.7		10448.4

In general, using the airport weather data underestimates the wind-driven rain on wall surfaces for all buildings except for Building 2. The largest error for Buildings No. 2, 3 and 6 is on the south wall by about 60%, while the largest error for Buildings No. 5 and 7 is on the north wall by about 90%. The significant error is due to the difference in wind direction. The prevailing wind direction during rain for the Vancouver International Airport is distinctly from the east while the prevailing wind direction for Buildings 2, 3 is between the east-north-east and east-south-east with a slightly higher frequency of wind from the east. For building 6, the prevailing wind direction during rain is from the east with a second highest frequency of wind from the south-south-east. For buildings 5 and 7, the prevailing wind direction is from the northeast.

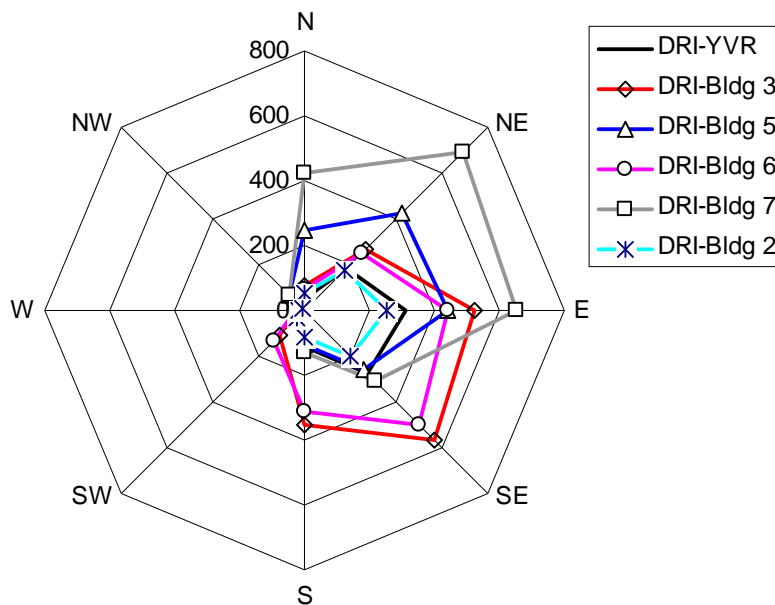


Figure 9. Comparison of airfield Driving Rain Index calculated using weather data collected on-site and from the Vancouver International Airport for the five monitored buildings.

Table 12 lists the errors in estimating wind-driven rain on four monitored buildings using weather data from the GVRD Burnaby South station. The terrain roughness factor T is assumed as 1.0 since the Burnaby South station is located in a similar urban area as the monitored buildings. The comparison

between the airfield Driving Rain Index calculated using weather data collected on site and from the Burnaby South station for Building 3 and Building 6 is shown in Figure 10.

Table 12. Errors in estimating wind-driven rain on four monitored buildings using weather data from the GVRD Burnaby South station for the monitoring period from January 1 to Sept. 30, 2007.

Orientation	DRI-Burnaby South station	DRI-Bldg. 3	error (%)	DRI-Bldg. 5	error (%)	DRI-Bldg. 6	error (%)	DRI-Bldg. 7	error (%)
N	97.2	77.6	25.3	248.9	-61.0	65.6	48.1	423.8	-77.1
E	421.4	524.0	-19.6	440.1	-4.2	438.7	-4.0	652.5	-35.4
S	381.8	350.0	9.1	106.9	257.2	314.5	21.4	126.9	200.8
W	27.0	31.6	-14.8	23.1	16.7	27.0	-0.2	18.9	42.7
Sum of error square			1321.1		70174.9		2792.3		49331.4

The accuracy of predicting wind-driven rain on wall surfaces for Building 3 and Building 6 is significantly increased by using weather data from the Burnaby South station, as the on-site wind and rain conditions are similar to that at the Burnaby South station. However, the errors for Buildings 5 and 7 are significantly increased, especially on the south wall due to the difference in prevailing wind direction. The prevailing wind direction at the Burnaby South station is from the east-south-east.

Table 13 lists the errors in estimating wind-driven rain on Building 2 using weather data from the GVRD Kitsilano station and Vancouver International Airport station. The comparison between the airfield Driving Rain Index calculated using weather data collected on site and from the Kitsilano station for Building 2 is shown in Figure 11. The Kitsilano station is located about 2.5 km away from Building 2. By using weather data from this station, the error is slightly decreased.

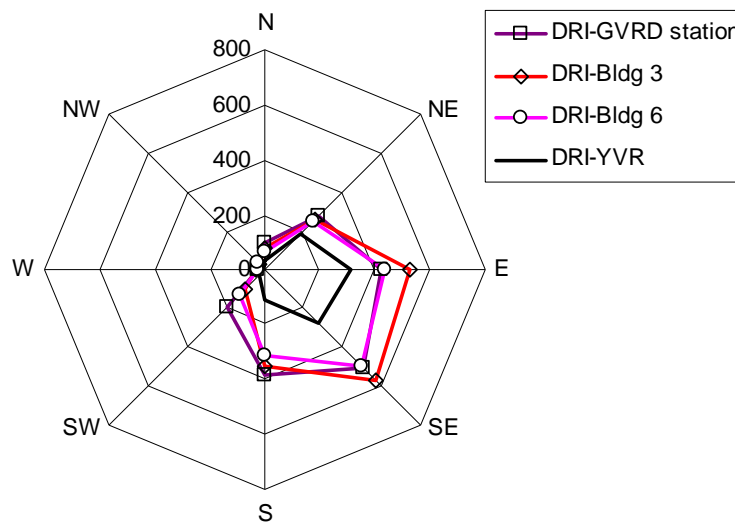


Figure 10. Comparison of airfield Driving Rain Index calculated using weather data collected on site and from the Burnaby South station for Building 3 and Building 6.

Table 13. Errors in estimating wind-driven rain on Building 2 using weather data from the GVRD Kitsilano station and Vancouver International Airport station for the monitoring period from January 1 to September 30, 2007.

Orientation	DRI-Building 2	DRI-Vancouver Airport station	error (%)	DRI-Kitsilano	error (%)
N	50.4	33.3	-33.9	54.9	9.0
E	252.3	310.9	23.2	326.3	29.3
S	80.1	111.7	39.5	76.1	-5.0
W	15.0	17.6	18.0	12.8	-14.5
Sum of error square			8559.6		3819.0

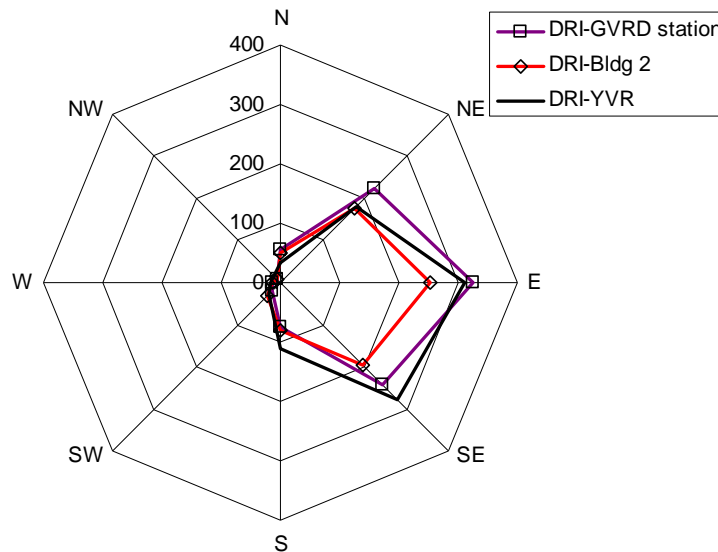


Figure 11. Comparison of airfield Driving Rain Index calculated using weather data collected on site and from the Vancouver International Airport and the Kitsilano station for Building No. 2.

5 Conclusions

The analyses of wind-driven rain data collected on the eight buildings indicated that the wind-driven rain exposure of a building site is significantly influenced by the local topography and surroundings. The airfield Driving Rain Index is only a relative indicator of the potential wind-driven rain exposure of a specific wall, and the actual amount of driving rain impinged on the surface is largely influenced by the building geometry and design details, i.e. overhang.

The prevailing wind direction varies from site to site. Buildings 2, 3, 5 and 7 are located in Vancouver. The prevailing wind direction is from the east with a slightly lower frequency of wind from the east-north-east for Buildings 2 and 3 and from the northeast for Buildings 5 and 7, although the wind direction at the Vancouver International Airport is distinctly from the east. For Buildings 1 (8), the prevailing wind direction is from the east-south-east, and for Building 6 the prevailing wind direction is from the east with a second highest frequency of wind from the south-south-east. In general, seasonal variation of wind directions is not significant.

The average wind speed recorded at 10 m above ground is less than 2 m/s for low-rise buildings, except for Building 3. Building 3 has a higher wind speed in the range of 2-4m/s, similar to the condition at the medium-height building site. The two high-rise buildings recorded an average wind speed slightly less than 4 m/s. Most of the time, wind speed is within the range of 2–6 m/s. In general, the average

wind speed is slightly higher during rain hours than during all hours; however, the maximum wind speed recorded during rain hours is lower than that during all hours. The average wind speed varies slightly over seasons and the winter has the highest wind speed. The recorded total amount of rainfall varies slightly from site to site. The average rainfall intensity recorded during the monitoring period falls under 2 mm/hr, which is consistent with the historical weather data (Levelton, 2006).

In general, the east and southeast facing walls have the highest wind-driven rain exposure. For some building sites monitored, walls facing the northeast and the north may receive a comparably high amount of rain. Therefore, these walls may have a higher risk of moisture damage due to the much lower solar radiation received on a north or northeast facing wall.

Because of the wind and rain characteristics in the coastal climate of BC, i.e., mild wind and light to moderate rain, the amount of driving rain impinged on the building surface is small compared to the literature data. The driving rain impinged on low-rise buildings with an overhang ratio of about 0.04 is only about 2–4% of the horizontal rainfall, and a significantly higher amount of 11% may be expected for low-rise buildings without any overhang. Higher buildings receive more driving rain, but not as high as may be perceived. For example, the 6-storey medium-height building receives an average amount of driving rain of about 15% of the horizontal rainfall, and the 16-storey high-rise building receives about 13% of the horizontal rainfall. These values may seem low compared to what has been normally perceived for higher buildings; however, Blocken (2004) confirmed through CFD modeling that higher buildings receive more driving rain on the upper part but much less or even none at the lower part due to the blocking effect. It is more so for mild wind conditions.

The measured data show that the overhang reduces wind-driven rain exposure by about four times for low-rise buildings and one and a half times for high-rise buildings for a small overhang with a ratio of 0.04. The protection area provided by the overhang seems to extend beyond 2.5m below the roof line for high-rise buildings and to half of the height for low-rise buildings. Given that the higher amount of driving rain received by high-rise buildings is due to the high rain deposition at the upper part of the building, while the lower part receives a small amount due to the blocking effect, the provision of an overhang may be effective for high-rise buildings in this particular climate.

The spatial distribution (catch ratio or wall factor) of wind-driven rain varies slightly over seasons due to the seasonal variation of wind speed. The rain deposition factor is normally the largest during the winter season, which exposes buildings to the highest amount of wind-driven rain in addition to the higher rainfall amount during the winter. The average wind-driven rain amount impinged on building surfaces is used for evaluating the long-term building envelope performance, while the wind-driven rain amount over a short period of heavy rain and strong winds is desirable in evaluating the rain penetration resistance of building envelope components.

The applicability of using an empirical method, the procedure prescribed by the British Standard BS-8104, to estimate the actual amount of wind-driven rain on specific wall surfaces is evaluated. The use of weather data reported from the Vancouver International Airport generally underestimates the amount of wind-driven rain received by all monitored buildings except for Building 2. The errors could be as much as 90% for north facing walls on Buildings 5 and 7 due to the difference in wind directions between the Vancouver International Airport and the building sites. The use of weather data from the close-by GVRD Burnaby South weather station significantly improves the accuracy in estimating the amount of wind-driven rain on Buildings 3 and 6. For Building 2, the use of weather data from the close-by Kitsilano station results in slightly better results than using the weather data from the airport station. Therefore, direct measurements of the rain impacting on building façades should be made wherever possible in the southern BC region, with significant local variation of wind and rain conditions. When direct measurements are not available, data from a weather station located in the

proximity of the building site with similar surroundings should be used, such as data collected from the GVRD's ambient air quality monitoring network. When weather data from the Vancouver International Airport is used for buildings in the Vancouver region, significant errors could be introduced, especially when the on-site prevailing wind direction is different from the prevailing wind direction at the airport station.

The unique set of wind-driven rain data generated through this project could be used for future work to validate CFD models in predicting the amount of wind-driven rain impacting on buildings in complex urban settings. Further work beyond the scope of this project may be required, for example, CFD modeling in order to evaluate quantitatively the effect of overhang and the possible optimum sizes.

6 References

1. Best, A. C. (1950). The size distribution of raindrops. *Quarterly Journal of Royal Meteorology Society*, 76 16-36.
2. Blocken, B. (2004). Wind-driven rain on buildings: measurements, numerical modeling, and application. Doctoral Thesis, Katholieke Universiteit Leuven, Belgium.
3. Blocken, B. and J. Carmeliet (2004). On the validity of the cosine projection in wind-driven rain calculations on buildings. *Building and Environment*.
4. BSI (1992). BS8104, Code of practice for assessing exposure of walls to wind-driven rain. British Standard.
5. CMHC (1996). Survey of building envelope failures in the coastal climate of British Columbia. Research report for Canadian Mortgage and Housing Corporation, Ottawa.
6. Ge, H. and Krpan, R. (2007). Field measurement of wind-driven rain on a low-rise building in the coastal climate of British Columbia. Proceedings of the 11th Canadian Conference on Building Science and Technology, March, Banff.
7. Inculet, D. and Surry, D. (1995). Simulation of wind driven rain and wetting patterns on buildings. Research report for Canadian Mortgage and Housing Corporation, Ottawa.
8. Laws J. and Parsons D. (1943). Relation of raindrop size to intensity. *Amer. Geophys. Union Trans*, 24, part II, pp. 453-460.
9. Levelton Engineering, Wind-Rain Relationships in Southwestern British Columbia – Final Report. Research report for CMHC, Ottawa, 2006.
10. Straube, J. and Burnett, E. (2000). Simplified prediction of driving rain on buildings. *Proceedings of the International Building Physics Conference*, Eindhoven University of Technology, Eindhoven, The Netherlands, pp. 375-382.
11. Straube (2006). Driving rain loads for Canadian building design. Research report for Canadian Mortgage and Housing Corporation, Ottawa.
12. Van Mook (2002). Driving rain on building envelopes. Ph.D. thesis. Building Physics Group, Eindhoven University of Technology, Eindhoven University Press, Eindhoven, The Netherlands, 198p.
13. WMO, World Meteorological Organization, Methods of correction for systematic error in point precipitation measurement for operational use (Sevruk B.), Operational Hydrology Report, WMO-No. 589, Geneva, 1982.

Appendix A

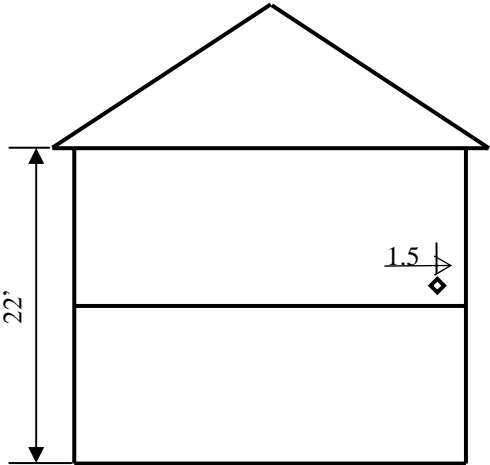
Building No. 1:

This is a two-storey single family house located on BCIT’s Burnaby Campus as a demonstration project. Two driving rain gauges were installed on the east façade, two on the west façade, and one on the south façade.

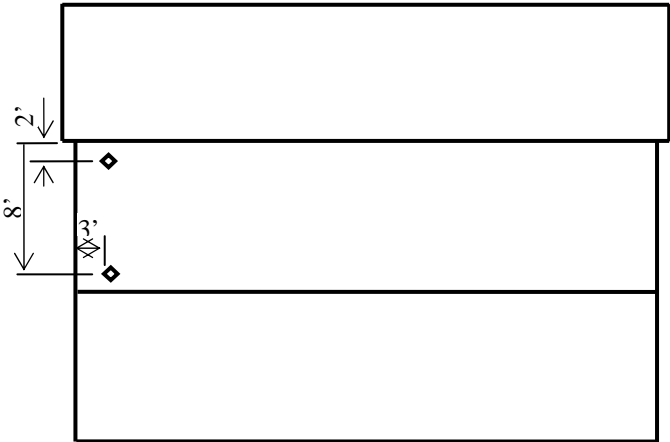


Figure A1. Satellite image of the surroundings of Bldg. 1.

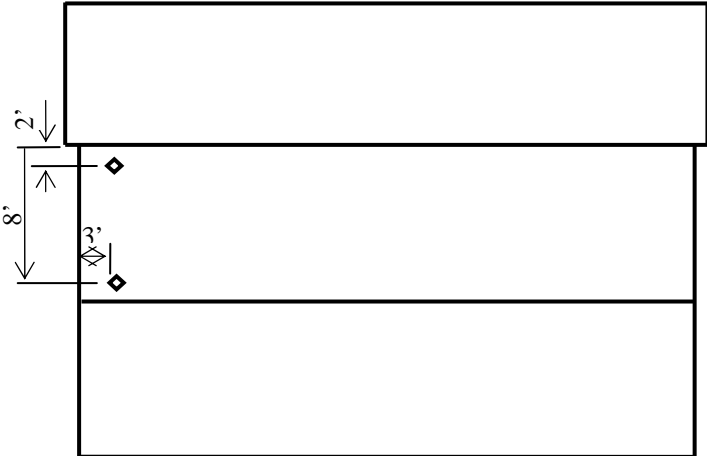
Figure A2. South façade of Bldg. 1.



1) South façade



2) East façade



3) West façade

Figure A3. Location of rain gauges on Bldg. 1.

Table A1. Spatial distribution of wind-driven rain on the façade of Bldg. 1 for the period from March 2007 to July 2008.

Driving rain gauge location	Catch Ratio					Wall factor averaged over the entire monitoring period
	Winter	Spring	Summer	Fall	Average over the entire monitoring period	
East-top	0.002	0.012	0.000	0.007	0.005	0.033
East-bottom	0.035	0.029	0.023	0.037	0.027	0.159
South	0.008	0.006	0.005	0.018	0.014	0.096
West-top	0.000	0.001	0.002	0.000	0.001	0.018
West-bottom	0.001	0.001	0.009	0.001	0.001	0.070

Building No. 2

This building is located close to the Jericho beach and surrounded by parks on the south and west sides. The east side is single-family buildings. There is no overhang. Six driving rain gauges were installed on this building: east façade (3), north (1), west (1), north-facing courtyard (1).

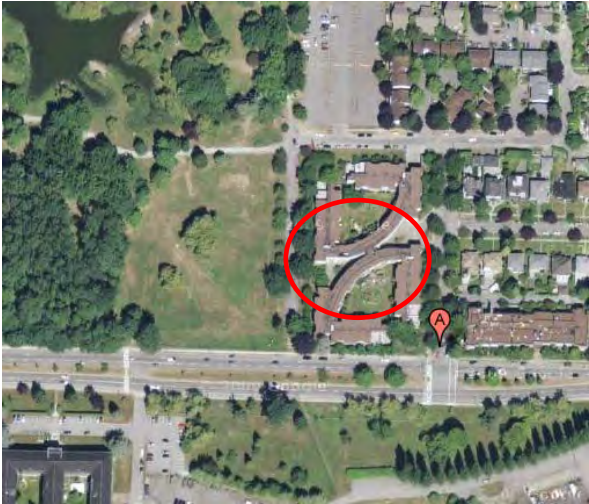
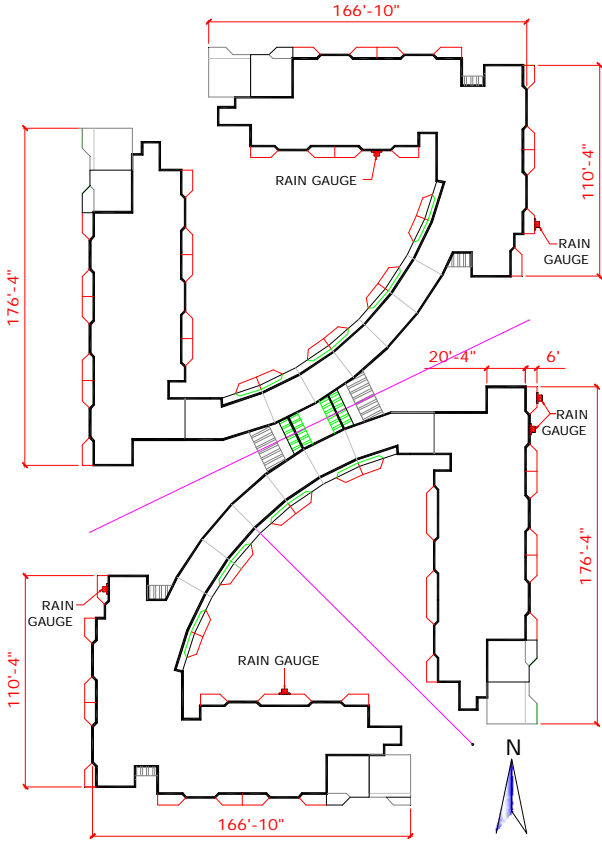


Figure A4: Satellite image of the surroundings of Bldg. 2. Figure A5. The north façade is facing a parking lot.



1) Plan view

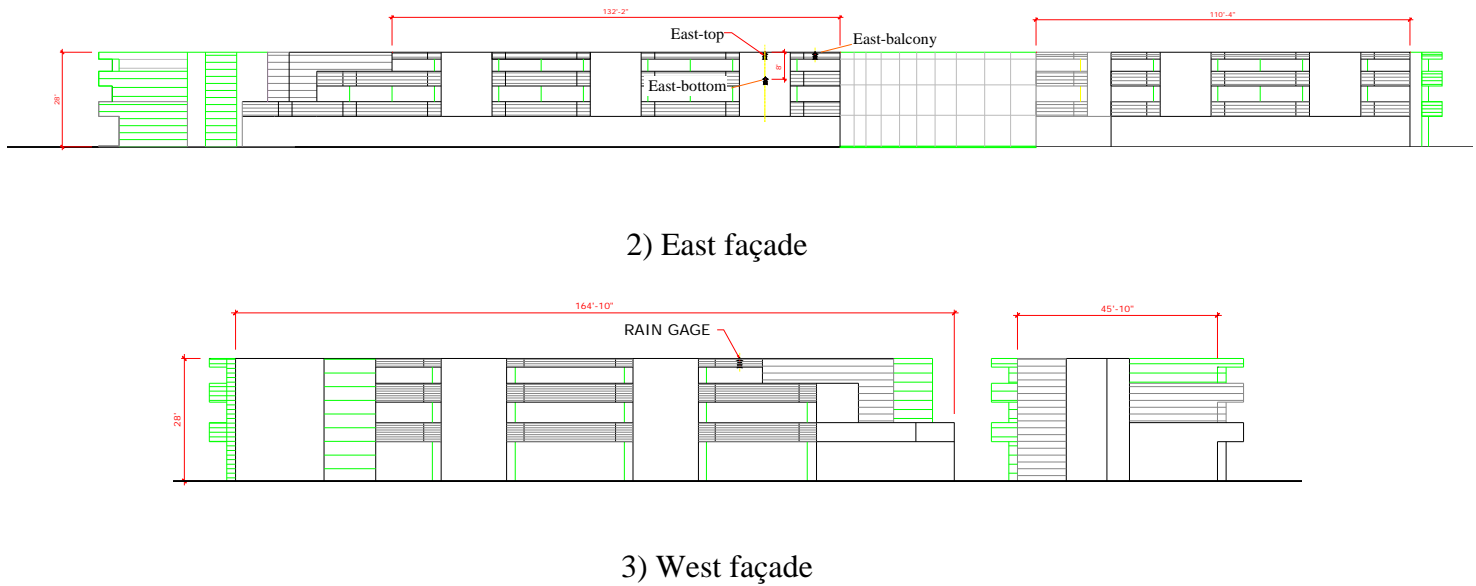


Figure A6. Location of rain gauges on Bldg. 2.

Table A2. Spatial distribution of wind-driven rain on the façade of Bldg. 2 for the period from November 2006 to July 2008.

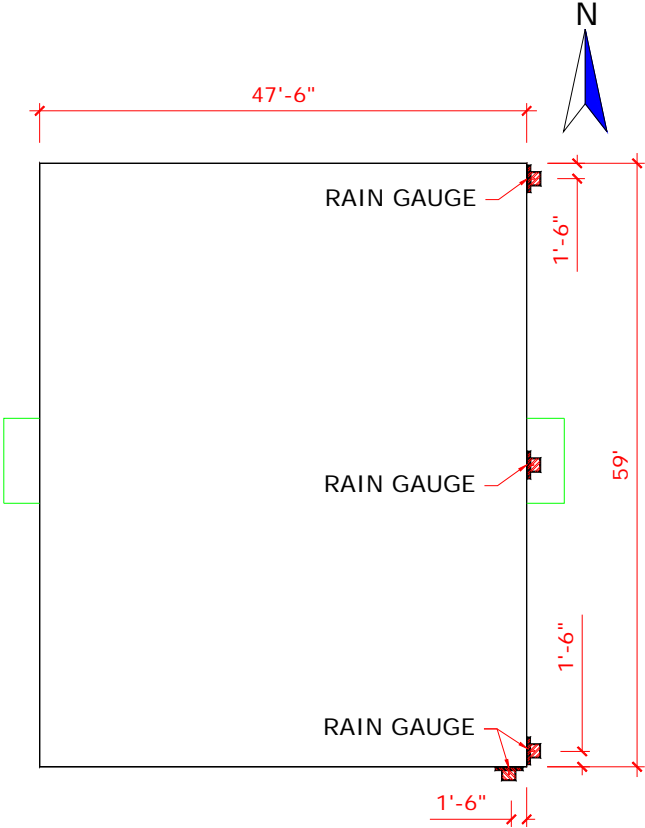
Driving rain gauge location	Catch Ratio					Average over the entire monitoring period	Wall factor averaged over the entire monitoring period
	Winter	Spring	Summer	Fall			
East-top	0.179	0.122	0.086	0.116	0.156	0.600	
East-bottom	0.097	0.057	0.035	0.056	0.079	0.308	
East-balcony	0.223	0.147	0.092	0.200	0.188	0.722	
West	0.063	0.105	0.188	0.053	0.050	0.432	
North	0.006	0.006	0.008	0.007	0.005	0.997	
Courtyard-North	0.020	0.019	0.010	0.017	0.019	0.409	

Building No. 3

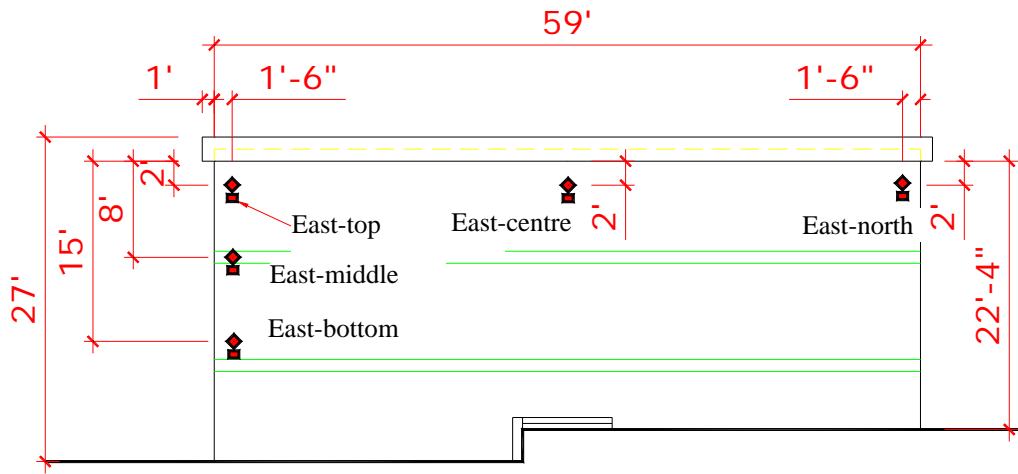
Building 3 is located in a block of 3-storey buildings with low-sloped roofs in a more open neighborhood. Six driving rain gauges were installed on this building, five on the east façade and one on the south façade.



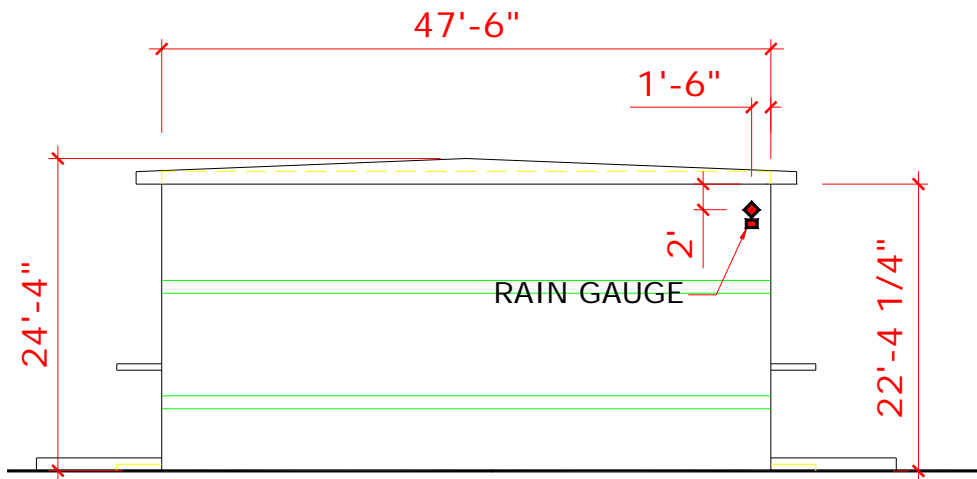
Figure A7. Satellite image of the surroundings of Bldg. 3. Figure A8. East façade of Bldg. 3.



1) Plan view



2) East façade



3) South façade

Figure A9. Location of rain gauges installed on Bldg. 3.

Table A3. Spatial distribution of wind-driven rain on the façade of Bldg. 3 for the period from November 2006 to July 2008.

Driving rain gauge location	Catch Ratio					Wall factor averaged over the entire monitoring period
	Winter	Spring	Summer	Fall	Average over the entire monitoring period	
East-top	0.007	0.001	0.000	0.006	0.004	0.008
East-middle	0.041	0.033	0.032	0.061	0.033	0.067
East-bottom	0.039	0.037	0.030	0.055	0.034	0.078
East-center	0.001	0.000	0.000	0.001	0.001	0.002
East-north	0.007	0.001	0.000	0.004	0.005	0.009
South	0.035	0.010	0.004	0.027	0.011	0.068

Building No. 4:

This building is located beside the Fraser River. Four driving rain gauges were installed, three on the southwest façade and one on the corner of the southeast façade.



Figure A10. Satellite image of the surroundings of Bldg. 4.



Figure A11. Southeast façade.



Figure A12. Location of rain gauges installed on Bldg. 4

Table A4. Spatial distribution of wind-driven rain on the southeast and southwest façades of Bldg. 4 for the period from March 2007 to July 2008.

Location	Southwest top	Southwest middle	Southwest corner	Southeast corner
Catch ratio	0.024	0.006	0.008	0.098

Note: The amount of horizontal rainfall collected during the same period from a close by GVRD weather station located in Burnaby south region is used for the calculation of the catch ratio.

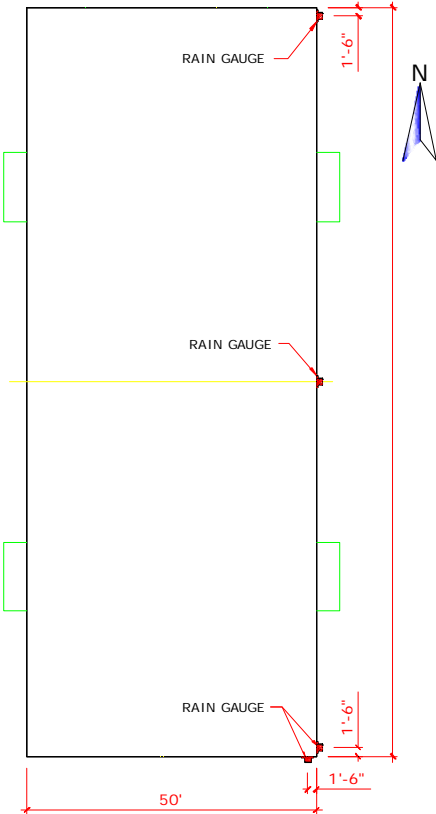
Building No. 5

This is a six-storey concrete building without overhang located on a small hill. The surroundings include several three-storey buildings to the north and the southeast slightly downhill towards Lougheed Highway. Six gauges were installed, five on the east side and one on the south side.



Figure A13. Satellite image of the surroundings of Bldg. 5.

Figure A14. Northwest corner of Bldg. 5.



1) Plan view

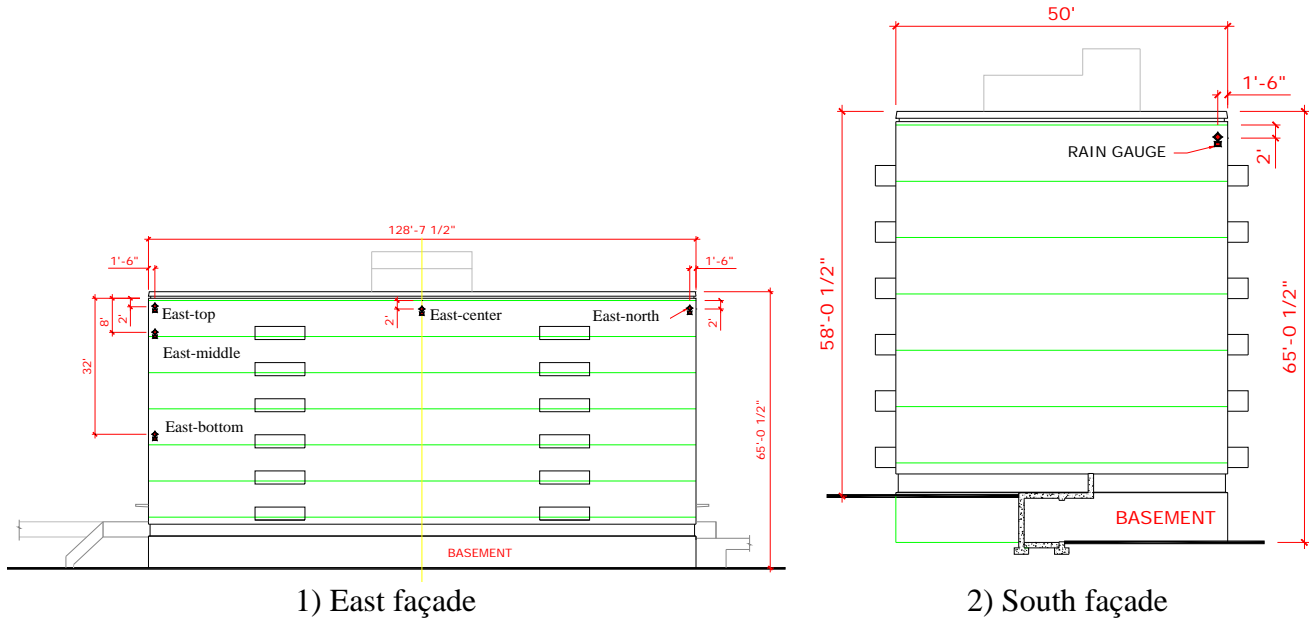


Figure A15. Location of rain gauges installed on Bldg. 5.

Table A5. Spatial distribution of wind-driven rain on the east and south façades of Bldg. 5 for the period from January 2007 to July 2008.

Driving rain gauge location	Catch Ratio				Average over the entire monitoring period	Wall factor averaged over the entire monitoring period
	Winter	Spring	Summer	Fall		
East-top	0.289	0.193	0.196	0.233	0.218	0.511
East-middle	0.224	0.154	0.168	0.162	0.168	0.432
East-bottom	0.100	0.062	0.065	0.082	0.074	0.209
East-center	0.416	0.320	0.404	0.244	0.324	0.716
East-north	0.436	0.309	0.373	0.356	0.371	0.732
South	0.164	0.105	0.087	0.101	0.116	0.930

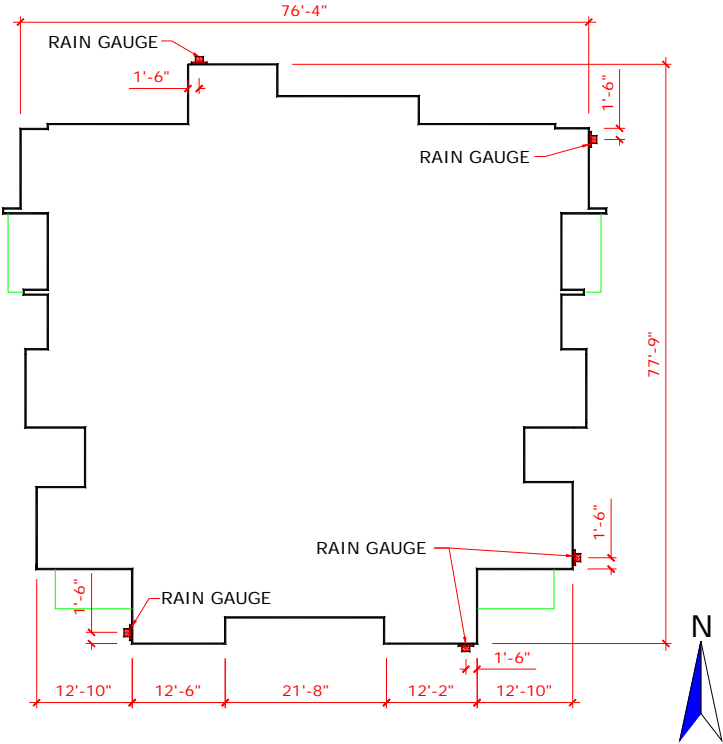
Building No. 6

This is a 16-storey residential building. Cladding includes areas of brick veneer and of CIP concrete. The surroundings include several high-rise buildings to the west and northeast, but the building is relatively unshielded to the south. The building is on the top of the Metrotown ridge in Burnaby and looks south downhill towards the Fraser River. Eight driving rain gauges were installed: east (5), south (1), north (1), and west (1).

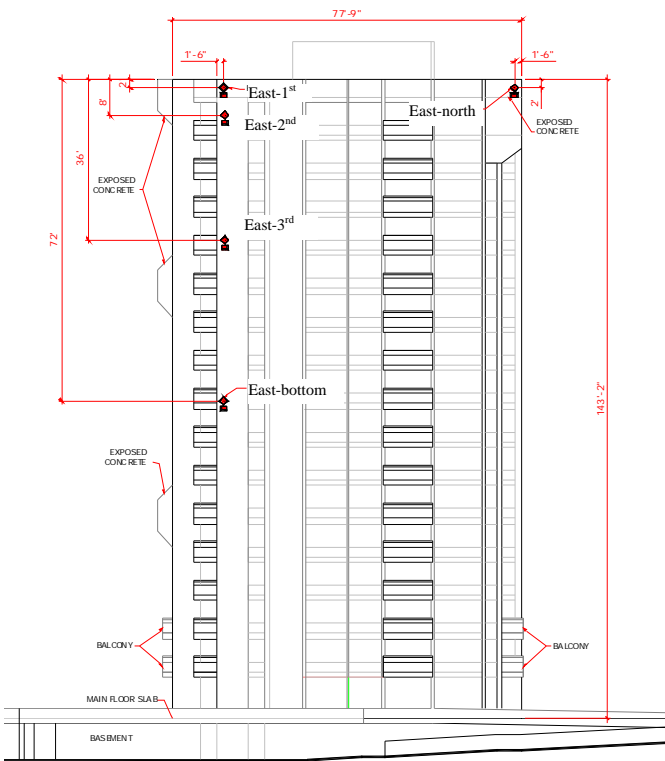


Figure A16. Satellite image of the surroundings of Bldg. 6.

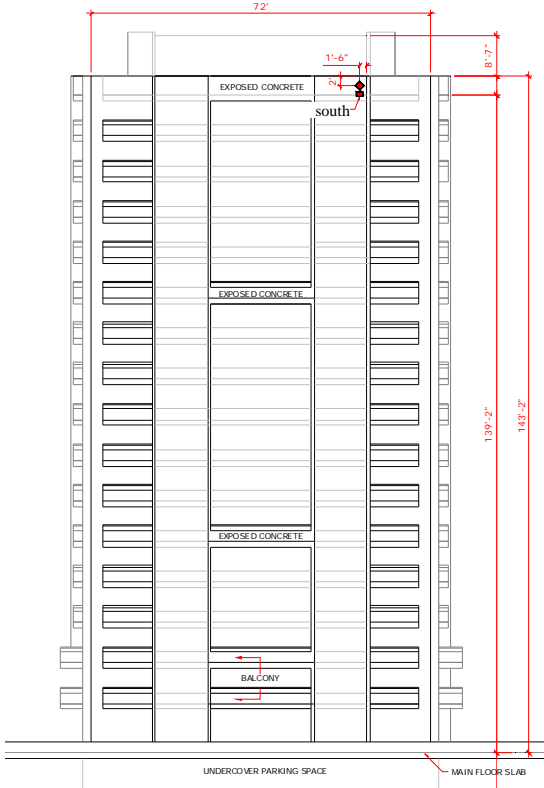
Figure A17. East façade of Bldg. 6.



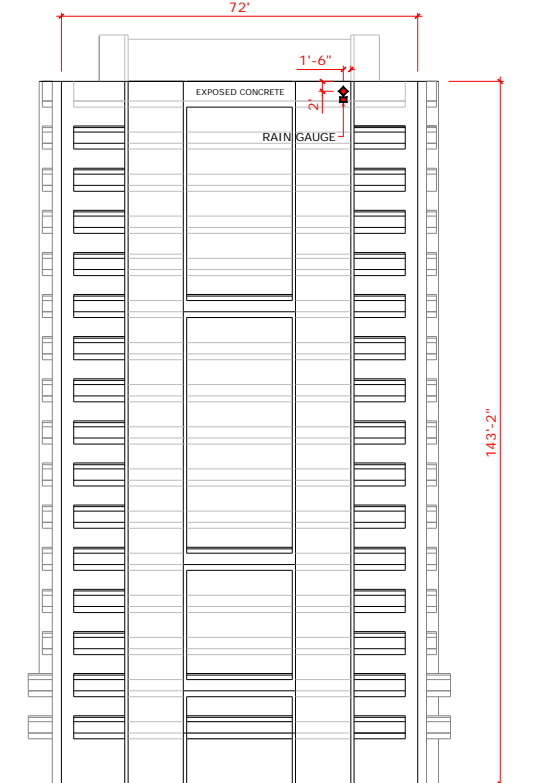
1) Plan view



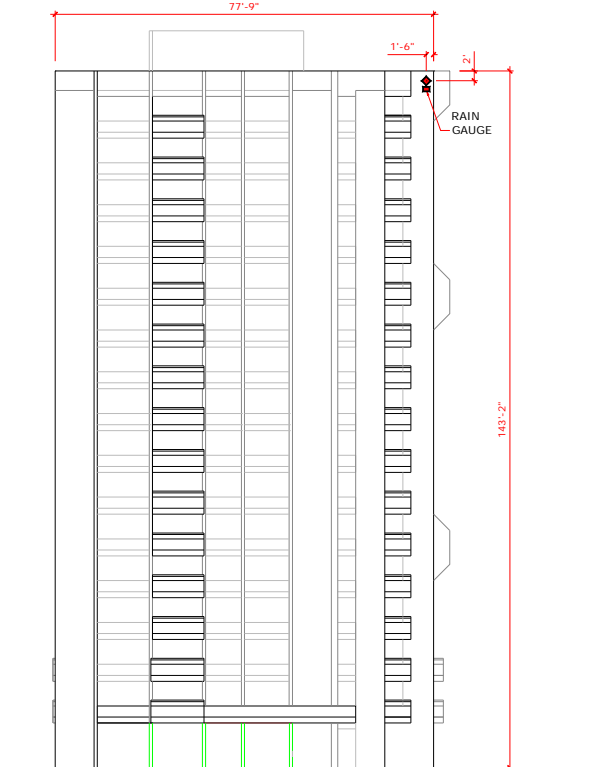
2) East façade



3) South façade



3) North façade



4) West façade

Figure A18. Location of rain gauges installed on Bldg. 6.

Table A6. Spatial distribution of wind-driven rain on the façade of Bldg. 6 for the period from December 2006 to July 2008.

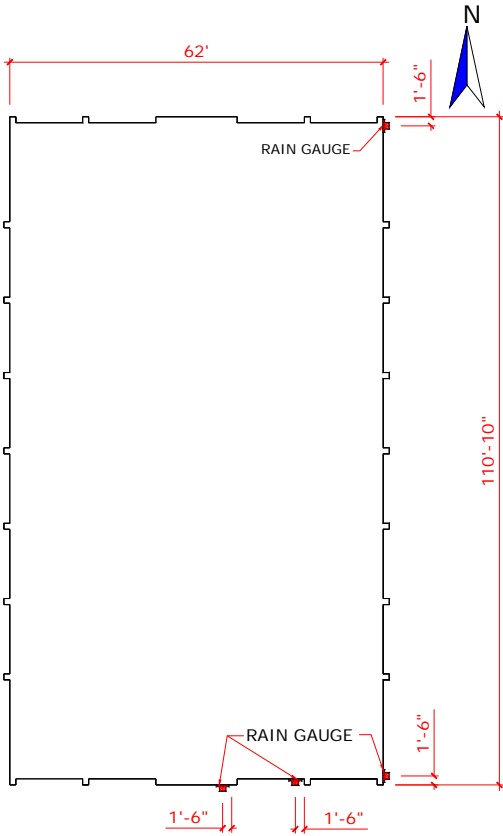
Driving rain gauge location	Catch Ratio					Average over the entire monitoring period	Wall factor averaged over the entire monitoring period
	Winter	Spring	Summer	Fall			
East-1st	0.368	0.246	0.212	0.287	0.304	0.501	
East-2nd	0.263	0.131	0.114	0.181	0.184	0.326	
East-3rd	0.112	0.057	0.047	0.061	0.081	0.143	
East-bottom	0.060	0.031	0.033	0.044	0.043	0.084	
East-north	0.215	0.133	0.110	0.177	0.175	0.289	
South	0.158	0.126	0.088	0.183	0.153	0.275	
West	0.029	0.034	0.068	0.038	0.033	0.446	
North	0.058	0.038	0.032	0.076	0.051	0.502	

Building No. 7

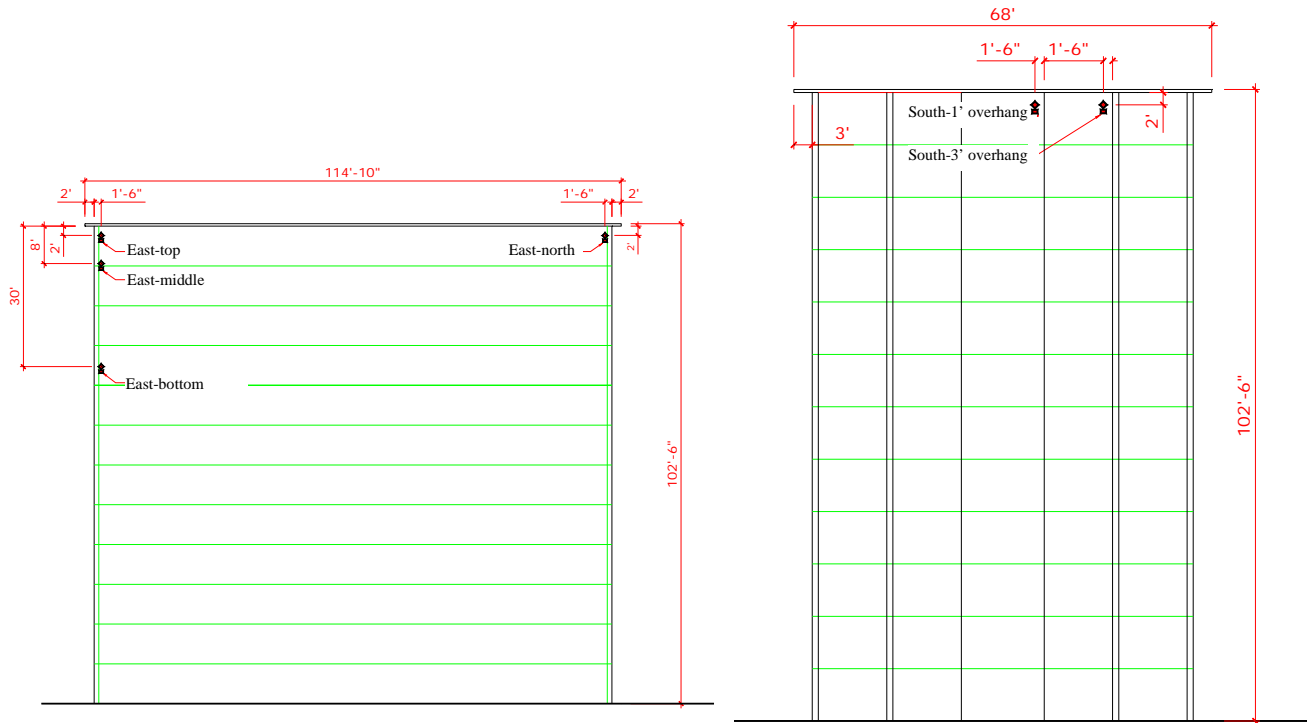
This is a 12-storey high-rise building with a 3' overhang. The building is located in a typical urban area surrounded by low-rise buildings. Six driving rain gauges were installed, four on the east façade and two on the south façade.



Figure A19. Satellite image of the surroundings of Bldg. 7. Figure A20. Northeast corner of Bldg. 7.



1) Plan view



2) East façade

3) South façade

Figure A21. Location of rain gauges on Bldg. 7.

Table A7. Spatial distribution of wind-driven rain on the façade of Bldg. 7 for the period from December 2006 to July 2008 excluding data from March, April and May 2008 due to the failure of the data logger.

Driving rain gauge location	Catch Ratio					Average over the entire monitoring period	Wall factor averaged over the entire monitoring period
	Winter	Spring	Summer	Fall			
East-top	0.024	0.003	0.003	0.029	0.012	0.022	
East-middle	0.105	0.063	0.058	0.099	0.087	0.119	
East-bottom	0.076	0.085	0.038	n/a*	0.074	0.112	
East-north	0.035	0.006	0.004	0.021	0.013	0.025	
South-1' overhang	0.012	0.006	0.003	0.025	0.009	0.259	
South-3' overhang	0.038	0.030	0.036	0.034	0.035	0.092	

*Driving rain gauge was blocked by dirt during this time period.

Building No. 8

This is a one-storey low aspect ratio building with 1/2' overhang on the BCIT Burnaby Campus. A weather pole is located in the parking lot in front of the building. Wind conditions are measured at 10 m above ground and horizontal rainfall is measured at 2 m above ground.



Figure A22. Satellite image of the surroundings of Bldg. 8.

Figure A23. East façade of Bldg. 8.

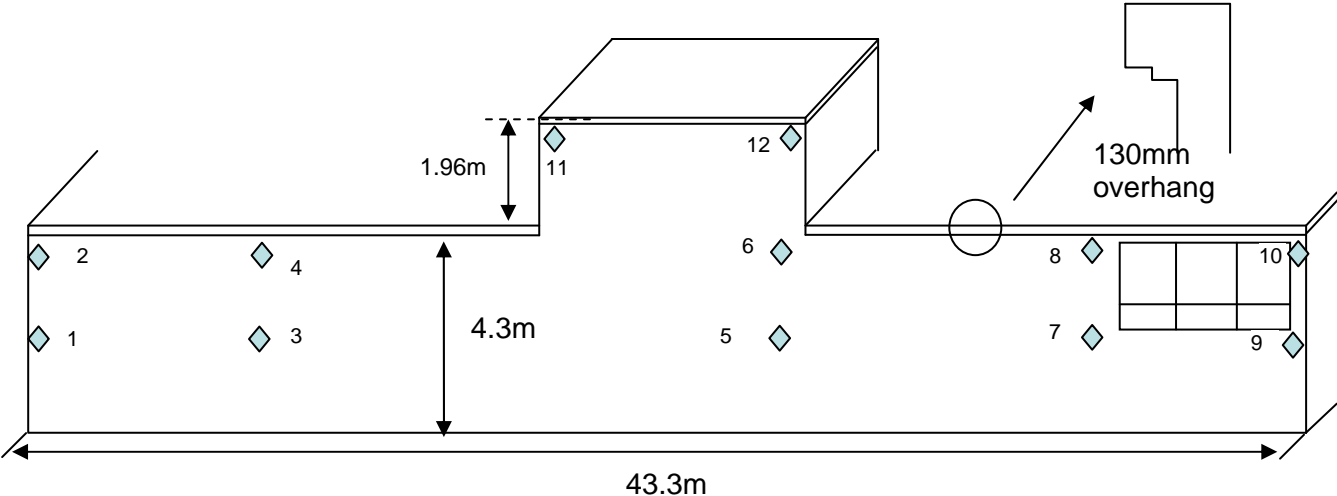


Figure A24. Location of rain gauges installed on the east façade of Bldg. 8.

Table A8. Spatial distribution of wind-driven rain on the east façade of Bldg. 8 for the period from March 2007 to July 2008.

Driving rain gauge location	Catch Ratio					Average over the entire monitoring period	Wall factor averaged over the entire monitoring period
	Winter	Spring	Summer	Fall			
1	n/a*						n/a*
2	n/a*						n/a*
3	0.031	0.037	0.027	0.045		0.035	0.264
4	n/a*						n/a*
5	0.032	0.038	0.024	n/a*		0.035	0.261
6	0.039	0.051	0.046	0.060		0.057	0.391
7	0.034	0.051	0.037	n/a*		0.048	0.360
8	0.044	0.040	0.021	0.046		0.031	0.209
9	n/a*	0.034	0.052	0.002		0.042	0.314
10	0.031	0.025	0.015	0.033		0.018	0.122
11	0.013	0.009	0.002	n/a*		0.010	0.076
12	0.025	0.017	0.008	0.024		0.011	0.064

*Driving rain gauge failure during this time period.